

Author Comments for Editor

ACP Discussions: acpd-15-9941-2015

(Editor - Federico Fierli)

‘Impact of different Asian source regions on the composition of the Asian monsoon anticyclone and on the extratropical lowermost stratosphere’

We thank the Editor Federico Fierli for encouraging the submission of a revised manuscript. We prepared and submitted a substantially revised version of our manuscript and are confident that we have satisfactorily addressed all comments of referee s#1 to #3. A detailed point-by-point response to all referee comments (#1 to #3) is attached. Further, a document specifying all changes in the revised manuscript compared to the ACPD version is added. Because substantial changes were performed in the revised manuscript, we give a brief summary below to make it easier to follow all changes.

1) In response to the comments of referee #3, we split the paper and elaborated a revised version of the ACPD paper with the focus on ‘The chemical composition of the air within and around the anticyclone with respect to the geographical sources of pollutants, and its temporal evolution’. We removed the other parts of the paper related to first, ‘the variation in shape of the Asian monsoon anticyclone’ and second, ‘the vertical/horizontal transport pathways out of the anticyclone’ in the revised version. We plan to publish these other parts of the ACPD paper in two separate publications. In the revised version of the paper, more analytic comparisons between CLaMS results and both MLS measurements and PV are presented.

2) In response to the comments of referee #1, we performed additional statistical analysis. Pattern correlation coefficients between CLaMS results and both MLS CO and O₃ measurements and PV are calculated (see Figs. 4 and 5, revised Version submitted to ACP) for the entire monsoon season 2012. Snapshots of CO and O₃ measured by MLS and simulated by CLaMS are shown in the Supplement of the paper. A main point of criticism of referee #1 was about our results identifying 2 modes (symmetric and asymmetric

states). We removed this part in the revised version of the paper. However, following the suggestion of referee #1, we have already started to perform further statistical analysis (EOF) to confirm our results.

3) The evaluation of referee #2 is very positive and asks only for minor revisions. We added more details about ENSO and monsoon rainfall in summer 2012. Further, for clarification we removed the part about the eddy shedding event on 20 September because it is not important for the focus of the revised version of the paper. Instead of the 20 Sep 2012 an other date (12 Sep 2012) in September is chosen to illustrate the late-phase of the Asian monsoon anticyclone.

4) CLaMS results shown in the revised version are taken from an updated CLaMS simulation compared to the results presented in the ACPD Version using additional emission tracers for the tropical Pacific, Atlantic and Indian Ocean (see Fig. 1, Tab. 1, Fig. 8, revised Version submitted to ACP). This new model run shows that the emission tracer for the tropical Pacific Ocean has also a small impact to the composition of the Asian monsoon anticyclone and shows a strong increase after the breakup of the anticyclone (see Fig. 8). In this new model version all regions of the Earth's surface that contribute more than 5% to the composition of the Asian monsoon anticyclone are identified.

Author Comment to Referee #1

ACP Discussions: acpd-15-9941-2015

(Editor - Federico Fierli)

‘Impact of different Asian source regions on the composition of the Asian monsoon anticyclone and on the extratropical lowermost stratosphere’

We thank Referee #1 for further guidance on how to to revise our paper. Following the reviewers advice we added further statistical analysis in the revised version of our paper. Our reply to the reviewer comments is listed in detail below. Questions and comments of the referee are shown in italics.

General comments

This study concerns an important physical process and contains interesting hypotheses that could illuminate the role of the Asian summer monsoon anticyclone for the transport of boundary layer into the stratosphere. However, the analysis is incomplete and the manuscript is not suitable for publication in its present form. For the most part, the analysis is restricted to instantaneous ‘snapshots’ of constituent (tracer) concentrations and dynamical quantities, detailed descriptions of those snapshots, and speculation about the underlying dynamics. However, there is very little analysis performed that proves - or even demonstrates - that the speculation is meaningful. What the authors have are interesting hypotheses that can form the basis for analysis, but not much more. The Asian anticyclone is an extensively studied phenomenon that warrants careful analysis. Furthermore, the diagnostic tools necessary for such an analysis are readily available and long familiar to this field; there is no justification for settling for speculation and anecdotal evidence for such a mature subject. To provide further guidance, the Specific Comments that follow discuss the analysis that could support individual statements in the Abstract.

We agree that we show as example individual days (‘snapshots’) of the Asian summer monsoon period 2012 to illustrate some basic characteristics of the

anticyclone. We think that is very helpful because in the literature often only mean values of the Asian monsoon anticyclone for July/August are shown, which hides the strong day-to-day variability of the Asian monsoon anticyclone. Further, we want to emphasise that as an addition animations showing the temporal evolution (on a daily basis) of the contribution of emission tracers for India/China and PV at 380 K potential temperature on the Northern Hemisphere during the Asian monsoon season 2012 (1 May 2012 - late October 2012) are available as a Supplement of this paper showing the intraseasonal variability of the Asian monsoon anticyclone. Most importantly, the main result of the paper is the intraseasonal variation of the contribution of different boundary source regions to the composition of the Asian monsoon anticyclone (Fig. 8, ACPD vers. + rev. vers.), which is performed over the whole period and not only for single days. Finally, in response to the reviewers comments, we have added two new figures to the paper (Fig. 4+5, rev. vers.) in which CLaMS results are compared with observations and PV from ERA-Interim over the entire monsoon period using pattern correlations.

Specific comments

1) Abstract, lines 5-9: Regarding the statement: ‘Our simulations show that the Asian monsoon anticyclone is highly variable in location and shape and oscillates between 2 states: first a symmetric anticyclone and second, an asymmetric anticyclone either elongated or split in two smaller anticyclones.’ To demonstrate this behavior, the authors show 4 snapshots of tracer concentrations and potential vorticity with the claim that these snapshots are typical. I do not question the author’s contention that they observe these patterns often in the data. However, the human eye is often too adept at finding patterns. If the anticyclone is truly dominated by two patterns, those patterns will emerge from an EOF (or similar) analysis as the two leading modes.

First, we want again to point out that in the electronic supplement of the paper, animations are available that illustrate the oscillation between a symmetric anticyclone and an asymmetric anticyclone. However, we agree that a statistical analysis by Empirical Orthogonal Functions (EOF) could help to investigate the variability the spatio-temporal distribution of the emission tracer for India/China during the monsoon season in a more quantitative

way. Indeed, we did first tests of an analysis with EOFs addressing this issue. However, adding an EOF analysis to our paper would extend the paper considerably and therefore would go beyond the scope of this paper. However, as also recommended by Reviewer #3, we plan to write a separate paper with additional statistical analysis to show our results regarding the oscillation (2 modes) of the anticyclone in 2012. Therefore, we removed the following part of the abstract and all other paragraphs within the paper related to this point.

✓ The following paragraph in the abstract is removed in the revised version of the paper:

‘The Asian monsoon anticyclone ... oscillates between 2 states: first a symmetric anticyclone and second, an asymmetric anticyclone either elongated or split in two smaller anticyclones. A maximum in the distribution of air originating from Indian/Chinese boundary layer sources is usually found in the core of the symmetric anticyclone, in contrast the asymmetric state is characterised by a double peak structure in the horizontal distribution of air originating from India and China.’

2) Abstract, lines 9-14: Regarding the statement: ‘A maximum in the distribution of air originating from Indian/Chinese boundary layer sources is usually found in the core of the symmetric anticyclone, in contrast the asymmetric state is characterised by a double peak structure in the horizontal distribution of air originating from India and China.’ An EOF analysis would work here as well. Also, if the two modes are separated via an EOF analysis of PV, then the structures of tracers that accompany those PV patterns will be revealed by projecting tracer variations onto the principal components of each PV EOF.

As mentioned before, we agree that a statistical analysis by Empirical Orthogonal Functions (EOF) will help to investigate the variability the spatio-temporal distribution of the emission tracer for India/China during the monsoon season, however to add an EOF analysis to our paper would extend the paper to much. However, we did address this point raised by the reviewer, albeit on a somewhat different way: we calculated the correlation between the horizontal distribution of PV to the spatial distribution of the emission tracer for India/China, Southeast Asia and CLaMS CO at 380 K (here Fig.1

= Fig. 5, rev. vers.)

✓ We added the following text and Figure 1 to Section 3.:

‘To link the temporal variation of the spatial distribution of the emission tracers also to areas of low PV during the entire Asian monsoon period 2012, pattern correlation between PV and the emission tracer for Indian/China (red), the emission tracer Southeast Asia (grey) and CLaMS CO (blue) are calculated as shown in Fig. 1. The correlation coefficients are calculated in a region between 15 and 50 N and 0 and 140 E (shown as black box in Fig. 2; ACPD paper) at 380 K similar as for the MLS/CLaMS correlations described above (above in the revised version of the paper, here see next point 3.). CLaMS results and PV are interpolated on 1×1 latitude longitude grid at 380 K and thereafter normalised to one.

Fig. 1 shows that the spatial distribution of PV and CLaMS CO is very well correlated during the formation (-0.89 to -0.95) and the existence (-0.74 to -0.93) of the Asian monsoon anticyclone. After the breakup the correlation gets worse. During the Asian monsoon season, a good correlation between the spatial distribution of low PV and high percentages of the emission tracer for India/China of -0.71 – -0.87 is calculated. During the formation of the anticyclone the correlation coefficients increases because the emission tracer has to be transported up to the UTLS. The decrease of the correlation coefficients after the breakup is caused by the missing convection in Asia occurring during the monsoon season (see comparison between MLS and CLaMS in Sect. 3.1.1). In contrast, the correlation coefficient between the spatial distribution of PV and the emission tracer for Southeast Asia shows a completely different behaviour. During the formation of the Asian monsoon the contributions of the emission tracer for Southeast Asia increase similarly as for the emission tracer for India/China. During the existence of the anticyclone a high correlation coefficient up to -0.90 is calculated at the early- and late-phase of the anticyclone, however in early August (mid-phase) no correlation between the spatial distribution of PV and the emission tracer for Southeast Asia is found (indicated by the grey dotted line in Fig. 1). This shows that in the mid-phase the spatial distribution of air masses originating in Southeast Asia is not connected to region of the Asian monsoon anticyclone indicating that air masses from Southeast Asia experienced upward transport outside of the Asian monsoon anticyclone (see Sect. 3.2).

The good correlation found between the emission tracer for India/China

and MLS measurements as well as PV confirms that the spatial distribution of the emission tracer for India/China is a very good proxy for the location and shape of Asian monsoon anticyclone from end-June to end-September.’

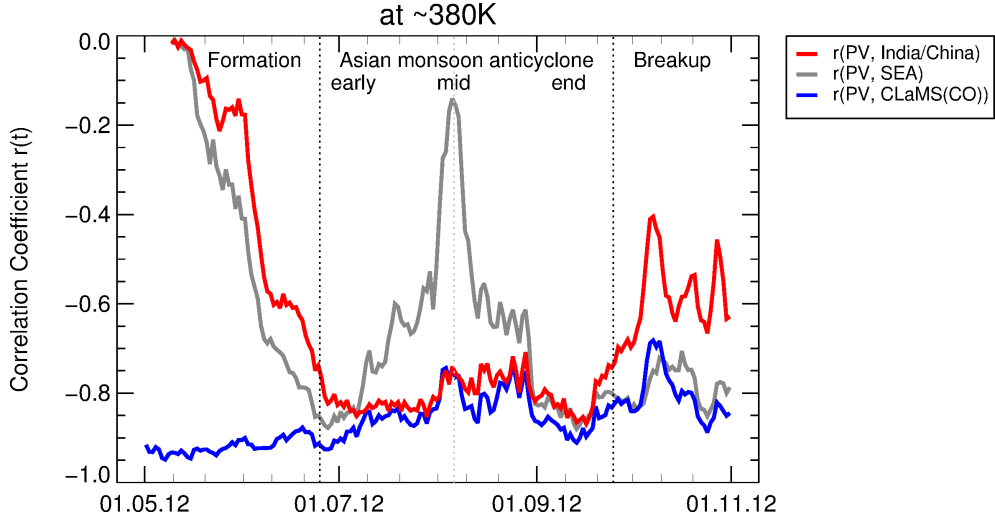


Figure 1: Time dependent correlation coefficients for the spatial distribution between PV and the emission tracer for India/China (red), the emission tracer for Southeast Asia (grey), and CLaMS CO (blue) at 380 K potential temperature. (added to the revised version of the paper as new Fig. 5)

3) *Abstract, lines 14-17: Regarding the statement: ‘The simulated horizontal distribution of artificial emission tracers for India/China is in agreement with patterns found in satellite measurements of O₃ and CO by the Aura Microwave Limb Sounder (MLS).’ The pattern agreements can be easily verified via pattern correlations - which should be performed for the entire season, not just 4 days.*

✓ Following the reviewers advice, we performed pattern correlation between MLS and CLaMS for the entire monsoon season 2012.

We revised Section 3.1.1 as follows:

Comparison to MLS measurements

‘To compare our simulation with MLS O_3 and CO measurements (Version 3.3) (Livesey et al., 2008), pattern correlation between MLS measurements and CLaMS results, namely $MLS(CO)/CLaMS(CO)$, $MLS(O_3)/CLaMS(O_3)$ and $MLS(CO)/CLaMS(India/China)$, were calculated (see Fig. 2). It is expected from satellite measurements that CO mixing ratios are stronger within the Asian monsoon anticyclone than outside and vice versa for O_3 indicating that air masses inside the anticyclone have a higher tropospheric characteristic than air masses in the UTLS outside of the anticyclone. At all days between 1 May 2012 and 31 October 2012, MLS measurements of O_3 and CO in a region between 15 and 50 N and 0 and 140 E (shown as black box in Fig. 2) at 380 ± 20 K potential temperature are correlated to CLaMS results as described in the following. At each day, CLaMS results are interpolated on locations of the MLS measurements transformed to synoptic 12:00 UTC positions. For each day, both MLS measurements and CLaMS results are normalised so that the maximum value of each trace gas is equal one. Afterwards the linear Pearson correlation coefficient $r(t)$ between MLS measurement and CLaMS results is calculated for each day. This procedure allows to be compared the spatial distribution of trace gases neglecting possible differences in the absolute mixing ratios between model and measurement and to compare the spatial distribution of different quantities such as measured CO and simulated emission tracers (here India/China).

Correlation coefficients $r(t)$ ranging between 0.72-0.86 were calculated for $MLS(O_3)/CLaMS(O_3)$ during the monsoon season 2012 between end of June and end of September. Before the monsoon season in early May an even higher correlation coefficient up to 0.95 was found. Correlation coefficients of 0.57-0.81 were calculated between both $MLS(CO)/CLaMS(CO)$ and $MLS(CO)/CLaMS(India/China)$ between end of June and end of September. These high correlation coefficients confirm that CLaMS has the capability of simulating the spatial distribution of tropospheric trace gases such as CO and stratospheric trace gases like O_3 measured by MLS. To illustrate this, the same horizontal cross-sections as in Figs. 2 and 3 at 380 K potential temperature for MLS CO and O_3 as well as for CLaMS CO and O_3 are shown in the Supplement of this paper.

Thus, high contributions of the emission tracers for India/China are simulated in regions where high values of CO are measured indicating that the

emission tracer for India/China is a good proxy for the spatial distribution of tropospheric trace gases measured in the region of the Asian monsoon anticyclone. The correlation coefficient of $\text{MLS}(\text{CO})/\text{CLaMS}(\text{India/China})$ increases from 0. to ≈ 0.8 during the formation of the Asian monsoon anticyclone, as expected because in the model the tracer has first to be transported from the ground to the UTLS. After the breakup of the monsoon anticyclone the correlation coefficient of $\text{MLS}(\text{CO})/\text{CLaMS}(\text{India/China})$ decreases because further upward transport of the tracer for India/China does not occur due to the missing convection in this region and therefore the spatial CO distribution in the UTLS is dominated by other processes. In the region of the Asian monsoon anticyclone, the correlation coefficients of $\text{MLS}(\text{O}_3)/\text{CLaMS}(\text{O}_3)$ are somewhat higher than those of $\text{MLS}(\text{CO})/\text{CLaMS}(\text{CO})$. Reasons for that could be deficiencies in MLS CO data (v3) in the lower stratosphere as suggested by Hegglin and Tegtmeier (2015). ’

Figures 4 and 5 in the ACPD paper were moved to the Supplement of the paper and were replaced by the following Figure 2:

4) Regarding the CLaMS simulations; Sec. 3.1.3 - 3.2.2: First, the analysis of transport paths is both anecdotal and speculative. The authors have a transport model; they should use it to perform focused analysis with model experiments designed to enlighten. Second, it seems clear from the upward trends of tracer concentrations in Fig. 8 that the CLaMS simulations have not spun up - that is, tracer concentrations in Fig. 8 are not true representations of actual concentrations. For example, there are potentially more tracers in the anticyclone in August than in June simply because those in August have had more time to get into the anticyclone - regardless of any physical transport process. In this context, it is still interesting that the SE Asia tracers dominate in June. Presumably this is because transport for those tracers is faster than for other regions. Nevertheless, that spin up is occurring during the analysis period makes that figure, and all CLaMS results very difficult to interpret.

First, CLaMS is a Lagrangian chemistry transport model and is very well suited to describe transport and mixing processes in the UTLS as shown in many previous studies (e.g. Pan et al., 2006; Konopka et al., 2010; Vogel et al., 2011; Konopka and Pan, 2012; Ploeger et al., 2013). Second, chemical trace gases in the model are initialised by satellite measurement and

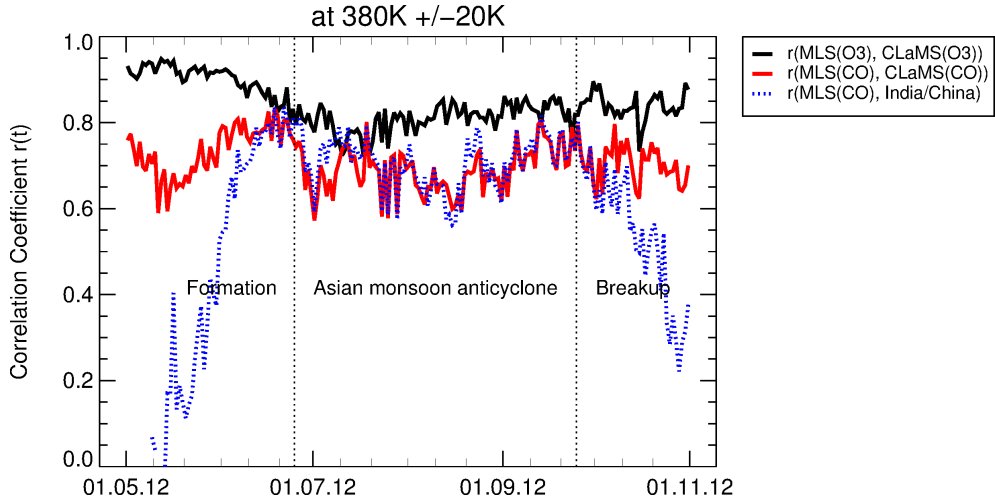


Figure 2: Correlation coefficients depending on time for tracer correlations patterns between MLS O_3 and CLaMS O_3 (black), between MLS CO and CLaMS CO (red), and between MLS CO and the CLaMS emission tracer for India/China (blue) for levels of potential temperature between 360 and 380 K (more details see text).

by results of a multi-annual CLaMS simulation started on 1 October 2001 as described in Sect. 2.1. This procedure ensures that the concentrations of chemical trace gases such as CO or O_3 used as initialisation for the 1 May 2012 do not need a spin up. Therefore, CO and O_3 mixing ratios simulated with CLaMS correspond to actual measured concentrations. CLaMS simulated CO and O_3 values are now used more extensively in the revised version (see here Fig. 2)

In contrast to these chemical tracers, the artificial emission tracers in CLaMS are designed to identify possible boundary source regions in Asia that could contribute to the composition of the Asian monsoon anticyclone in a particular monsoon season. Thus, we argue that both in the model and in the real world it takes time for boundary tracers to reach the anticyclone in the early stages of the monsoon season. In response, to the review comment and to explain this in more detail we added the following paragraph in the revised version of the paper:

in Sect. 2.1.1 Model Description / Emission tracers:

‘The artificial emission tracers in CLaMS are designed to identify possible boundary source regions in Asia that could contribute to the composition of the Asian monsoon anticyclone in a particular monsoon season, here as a case study for the year 2012. At each time step of the model (every 24 hours) air masses in the model boundary layer are marked by the different emission tracers, i. e. the emission tracer for North India (NIN) of an air parcel in the boundary layer over Northern India is set equal to one ($NIN = 1$). If an air parcel has left the model boundary layer over North India, the value of the emission tracer for NIN ($=1$) is transported to other regions of the free troposphere or stratosphere. Successive mixing processes between air masses from North India with air masses originating in other regions of the atmosphere (here $NIN = 0$) during the course of the simulation yield values of NIN differing from the initial distribution ($NIN = 1$ or $NIN = 0$). Therefore, the value of the individual emission tracer count the percentage of an air masses that originated in the specific boundary layer region since 1 May 2012 considering advection and mixing processes.’

in Sect. 3.2.1 Temporal evolution of different emission tracer:

‘The artificial emission tracers in CLaMS are designed to identify possible boundary source regions in Asia that could contribute to the composition of the Asian monsoon anticyclone during the monsoon season 2012 (as defined in Sect. 2.1) considering advection and mixing processes. E. g. the fact that the contribution of the emission tracer for Southeast Asia dominates in June demonstrates that in June upward transport or convection in the region of Southeast Asia is stronger than in other regions over Asia causing higher contributions of the emission tracer of Southeast Asia within the Asian monsoon anticyclone compared to other emission tracers in June. By this technique contributions of the boundary layer with a transport time from the boundary to the UTLS longer than one monsoon period (contributions from the boundary layer that are released before 1 May 2012) are not covered by the artificial tracers used here. Therefore, the composition of different emission tracers within the Asian monsoon anticyclone is a fingerprint of the regional and temporal variations of convective processes causing strong upward transport within the Asian monsoon anticyclone in summer 2012.

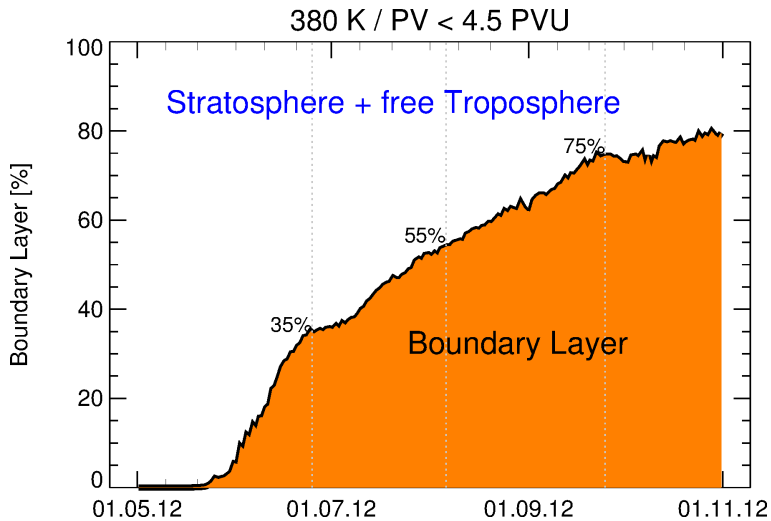


Figure 3: Temporal evolution of contributions of air masses from the boundary layer to the composition of the Asian monsoon anticyclone. The shown percentages are mean values calculated for air masses in Asia in the region between 15 and 50 N and 0 and 140 E at 380 ± 0.5 K (see black box in Fig. 1 in the paper) with PV values lower than 4.5 PVU that marks the edge of the anticyclone.

The sum of all emission tracers shown in Fig. 8 (ACPD vers.) is less than 100 % because air masses originating in the free troposphere or stratosphere also contribute to the composition of Asian monsoon anticyclone. End of June, a contribution of 35 % of the model boundary layer to the composition of the Asian monsoon anticyclone is calculated (see here Fig. 3). The remaining 65 % of the composition of the anticyclone is from the free troposphere and the stratosphere. The contribution of the model boundary layer rises to 55 % in early August and to 75 % at the end of the monsoon season in late September. ’

References

Hegglin, M. I., and Tegtmeier, S. (Eds.): SPARC Data Initiative: Assessment of Stratospheric Trace Gas and Aerosol Climatologies from Satellite Limb Sounders, SPARC Report No. 7, in preparation, 2015.

- Konopka, P. and Pan, L. L.: On the mixing-driven formation of the Extratropical Transition Layer (ExTL), *J. Geophys. Res.*, 117, D18301, doi:10.1029/2012JD017876, 2012.
- Konopka, P., Grooß, J.-U., Günther, G., Ploeger, F., Pommrich, R., Müller, R., and Livesey, N.: Annual cycle of ozone at and above the tropical tropopause: observations versus simulations with the Chemical Lagrangian Model of the Stratosphere (CLaMS), *Atmos. Chem. Phys.*, 10, 121–132, 2010.
- Livesey, N. J., Filipiak, M. J., Froidevaux, L., Read, W. G., Lambert, A., Santee, M. L., Jiang, J. H., Pumphrey, H. C., Waters, J. W., Cofield, R. E., Cuddy, D. T., Daffer, W. H., Drouin, B. J., Fuller, R. A., Jarnot, R. F., Jiang, Y. B., Knosp, B. W., Li, Q. B., Perun, V. S., Schwartz, M. J., Snyder, W. V., Stek, P. C., Thurstans, R. P., Wagner, P. A., Avery, M., Browell, E. V., Cammas, J.-P., Christensen, L. E., Diskin, G. S., Gao, R.-S., Jost, H.-J., Loewenstein, M., Lopez, J. D., Nedelec, P., Osterman, G. B., Sachse, G. W., and Webster, C. R.: Validation of Aura Microwave Limb Sounder O₃ and CO observations in the upper troposphere and lower stratosphere, *J. Geophys. Res.*, 113, D15S02, doi:10.1029/2007JD008805, 2008.
- Pan, L. L., Konopka, P., and Browell, E. V.: Observations and model simulations of mixing near the extratropical tropopause, *J. Geophys. Res.*, 111, doi:10.1029/2005JD006480, 2006.
- Ploeger, F., Günther, G., Konopka, P., Fueglistaler, S., Müller, R., Hoppe, C., Kunz, A., Spang, R., Grooß, J.-U., and Riese, M.: Horizontal water vapor transport in the lower stratosphere from subtropics to high latitudes during boreal summer, *J. Geophys. Res.*, 118, 8111–8127, doi:10.1002/jgrd.50636, 2013.
- Vogel, B., Pan, L. L., Konopka, P., Günther, G., Müller, R., Hall, W., Campos, T., Pollack, I., Weinheimer, A., Wei, J., Atlas, E. L., and Bowman, K. P.: Transport pathways and signatures of mixing in the extratropical tropopause region derived from Lagrangian model simulations, *J. Geophys. Res.*, 116, D05306, doi:10.1029/2010JD014876, 2011.

Author Comment to Referee #2

ACP Discussions: acpd-15-9941-2015

(Editor - Federico Fierli)

‘Impact of different Asian source regions on the composition of the Asian monsoon anticyclone and on the extratropical lowermost stratosphere’

We thank Referee #2 for his very good evaluation. Following the reviewers advice we elaborate some minor points, which strengthen the findings of our paper. Our reply to the reviewer comments is listed in detail below. Questions and comments of the referee are shown in italics.

This paper reports characteristics of monsoon anticyclone, impact of emissions from India, China and Southeast Asia on the composition of anticyclone and transport path- ways to the lower stratosphere. The results from CLaMS model are supported by MLS observations. This paper highlights new and important findings. I recommend the paper to be published in ACP after the following minor comments are addressed.

Minor comments

1. P9945, L27. The reason for choice of year 2012 should be mentioned. Was it El- Niño/La-Nina year? Or normal monsoon? Or QBO Easterly/westerly phase? These phenomena affect the monsoon circulation and therefore transport into monsoon anticyclone.

✓ The following text is added in the revised version of the paper:

‘The summer 2012 is a good example for normal monsoon conditions. The rainfall in India was normal based on the rainfall data set of 306 rain gauges in India provided by the Indian Institute of Tropical Meteorology in Pune, India (see <http://www.tropmet.res.in/~kolli/mol/Monsoon/Historical/air.html>). A strong relation between rainfall (droughts or floods) during the Indian summer monsoon to El Niño and La Niña events have been established (e.g.

Webster et al., 1998; Kumar et al., 2006). In summer 2012, neutral conditions for the El Niño/Southern Oscillation (ENSO) occurred based on the Oceanic Niño Index (ONI) (see <http://ggweather.com/enso/oni.htm>).

The relation of the Quasi-Biennial-Oscillation (QBO) in stratospheric equatorial winds to Indian summer monsoon rainfall is discussed in the last years (e.g. Chattopadhyay and Bhatla, 2001, International Journal of Climatology; Claud and Terray, 2007, Journal of Climate; Mohankumar and Pillai, 2008, Journal of Atmospheric and Solar-Terrestrial Physics), however there is no clear result to how the QBO is related to normal monsoon conditions. Therefore we decided that a discussion about the possible connection between QBO and Indian summer monsoon in the year 2012 should not be added to our paper.

2. Section 3.1.1 is very lengthy and should be shortened. The discussion on eddy shedding is not clear. ‘The second anticyclone moves towards Pacific Ocean along subtropical westerly jet’? Consider revising this.

✓ We shortened section 3.1.1. by removing the paragraph about the 2 modes (symmetric - antisymmetric) in the revised version of the paper. The paragraph about the eddy shedding is also removed.

3. P9957, L26. ‘On 20 September 2012 (see Fig. 7, bottom), the anticyclone is shifted to the south’. Is this related to monsoon withdrawal?

✓ In the revised version of the paper, we replaced the 20 September 2012 by 12 September 2012 to remove the discussion about the eddy shedding event, which is not important for the main message of the paper. During September a strong broadening of the spatial distribution of the emission tracer for India/China towards the tropics is found. This is likely related to the monsoon withdrawal as shown in the following new figure (Fig. 1) introduced in the revised version of the paper.

4. P9960 L10-11. Temporal evaluation of tracers in the anticyclone and its oscillation with 30-60 days periodicity show connections with movement of monsoon trough. This indicates that the lower level convergence (monsoon trough) and upper level divergence (anticyclone) vary coherently. The two anticyclones (Tibetan and Iranian mode) observed in MLS, which are simu-

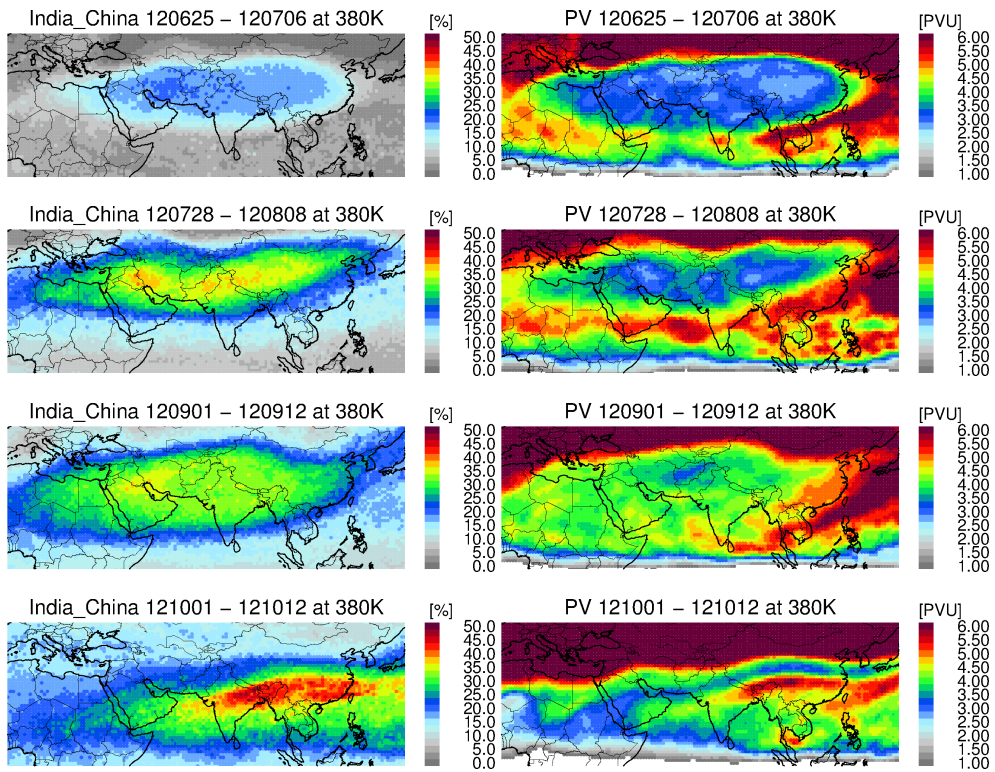


Figure 1: Twelve-day mean values of the contribution of the emission tracer for India/China (left) and PV (right) during four different phases of the Asian monsoon anticyclone: early-phase (top) , mid-phase (2nd row), end-phase (3rd row) of the anticyclone and after the breakup (bottom).

lated by CLaMs too, should have corresponding two low pressure areas in the lower troposphere. The figure depicting this will support your results

Our simulations show that a south-north shift in the contribution of different emission tracers for Asia within the Asian monsoon anticyclone occurred during the summer 2012 and also a slight northward shift of the anticyclone itself. This behaviour is possibly linked to the northward moving long-term interseasonal variations (30 to 60 day oscillations) found in climatological analyses of monsoon activity like convection and rainfall (e.g. Goswami, 2012, and references therein). The calculated composition of different emission tracers within the Asian monsoon anticyclone is a fingerprint of the regional and temporal variations of convective processes causing strong upward transport within the Asian monsoon anticyclone in summer 2012. However, in spite of a considerable effort analysing meteorological data set, we could not find any clear evidence that lower level convergence (monsoon trough) and upper level divergence (anticyclone) vary coherently. Therefore, we can not provide an appropriate figure. We agree that the connection between the movement of the lower level monsoon trough and the movement of the anticyclone is an interesting open question.

5. P9961 L8-9. Statement 'however the contributions of the different emission tracers are in general lower' is not clear

✓ We revised the following sentence

'Further, even if no PV criterion is applied and all air parcels within the geographical limits (black box in Fig. 7) are considered to calculate the mean values, the same qualitative evolution emerges of the contributions of different emission tracers within the anticyclone at 380 K, however the mean values of the single emission tracers are in general lower (not shown here).'

as follows:

'Further, even if no PV criterion is applied and all air parcels within the geographical limits (black box in Fig. 7 of the paper) are considered to calculate the mean values, the same qualitative evolution emerges of the contributions of different emission tracers within the anticyclone at 380 K, however then highest contributions from Southeast Asia up to 11% and 19% are calculated

in mid-June/mid-July and October, respectively. The contribution of air masses from North India are also at the maximum in the intervening period from mid-July to mid-August and reach values up to 13% (not shown here).'

6. Mean values of contributions of emission tracers for India/China, Southeast Asia, and Western Pacific etc should be mentioned in the conclusion section.

✓ We added the mean values as follows:

'In the early (\approx June to mid-July) and late period (\approx mid-August to October) of the monsoon season 2012, contributions from Southeast Asia are highest (up to 13% and 23%, respectively, using a value of 4.5 PVU to mark the edge of the anticyclone). In the intervening period (\approx mid-July to mid-August), air masses from North India have the strongest impact (up to 18%).'

7. P9968 L15-19. The high contribution from SE Asia in early May-June and late monsoon period (Sep-Oct) may due to migration of monsoon trough. During this period it is generally over SE Asia. Authors should confirm this and make an assertive statement.

See above point 4.)

References

- Goswami, B. N.: Intraseasonal Variability in the Atmosphere-Ocean Climate System, chap. 2: South Asian monsoon, pp. 21–72, Springer-Verlag Berlin Heidelberg, 2nd edn., editors: W. K. M. Lau and D. E. Waliser, 2012.
- Kumar, K. K., Rajagopalan, B., Hoerling, M., Bates, G., and Cane, M.: Unraveling the Mystery of Indian Monsoon Failure During El Niño, *Science*, 314, 115–119, doi:10.1126/science.1131152, 2006.
- Webster, P. J., Magaña, V. O., Palmer, T. N., Shukla, J., Tomas, R. A., Yanai, M., and Yasunari, T.: Monsoon: Processes, predictability, and the prospects for prediction, *J. Geophys. Res.*, 103, 14.451–14.510, 1998.

Author Comment to Referee #3

ACP Discussions: acpd-15-9941-2015

(Editor - Federico Fierli)

‘Impact of different Asian source regions on the composition of the Asian monsoon anticyclone and on the extratropical lowermost stratosphere’

We thank Referee #3 for this detailed and very helpful review. Following the reviewers advice we split the paper into three parts. Our reply to the reviewer comments is listed in detail below. Questions and comments of the referee are shown in italics.

General Remarks

The paper presents a model study of the Asian monsoon anticyclone; the development during the year 2012 from May to October is shown as a case study. The paper tackles a number of important topics:

1) the variation in the position and shape of the Asian monsoon anticyclone over the year from formation to break-up;

2) The chemical composition of the air within and around the anticyclone with respect to the geographical sources of the pollutants, and its temporal evolution;

3) the vertical and horizontal transport pathways out of the anticyclone, and potential transport barriers.

Over all, the paper is rather descriptive and wordy instead of analytical (in a quantitative sense) and concise. For none of the topics listed, the authors got to the bottom of the issue. For this reason, a leaner paper focussing on just one of these topics, but doing this more exhaustively, would have been probably more helpful. With such a wealth of material to analyse, the authors

should indeed think of splitting this paper into two or even three. However, this is fully at the decision of the authors

In response to this comment, we split the paper and elaborated a revised version of the paper with the focus on ‘The chemical composition of the air within and around the anticyclone with respect to the geographical sources of the pollutants, and its temporal evolution’. We removed the other parts of the paper in the revised version of the paper.

Some comparisons to satellite observations of trace gases are performed, however, these are by far not extensive. Thus, the presented results have mainly to be taken as model reality rather than real world

✓ For the revised version of the paper we performed pattern correlation between MLS measurements and CLaMS simulations in the regions of the Asian monsoon anticyclone for the entire monsoon season 2012 (1 May - 31 Oct 2012), and have added a new figures (Fig.4) with comparisons between CLaMS and MLS :

We revised Section 3.1.1 as follows:

’Comparison to MLS measurements

‘To compare our simulation with MLS O₃ and CO measurements (Version 3.3) (Livesey et al., 2008), pattern correlation between MLS measurements and CLaMS results, namely MLS(CO)/CLaMS(CO), MLS(O₃)/CLaMS(O₃) and MLS(CO)/CLaMS(India/China), were calculated (see Fig. 1). It is expected from satellite measurements that CO mixing ratios are stronger within the Asian monsoon anticyclone than outside and vice versa for O₃ indicating that air masses inside the anticyclone have a higher tropospheric characteristic than air masses in the UTLS outside of the anticyclone. At all days between 1 May 2012 and 31 October 2012, MLS measurements of O₃ and CO in a region between 15 and 50 N and 0 and 140 E (shown as black box in Fig. 2) at 380 ± 20 K potential temperature are correlated to CLaMS results as described in the following. At each day, CLaMS results are interpolated on locations of the MLS measurements transformed to synoptic 12:00 UTC positions. For each day, both MLS measurements and CLaMS results are normalised so that the maximum value of each trace gas is equal one. After-

wards the linear Pearson correlation coefficient $r(t)$ between MLS measurement and CLaMS results is calculated for each day. This procedure allows to be compared the spatial distribution of trace gases neglecting possible differences in the absolute mixing ratios between model and measurement and to compare the spatial distribution of different quantities such as measured CO and simulated emission tracers (here India/China). Correlation coefficients $r(t)$ ranging between 0.72-0.86 were calculated for $\text{MLS}(\text{O}_3)/\text{CLaMS}(\text{O}_3)$ during the monsoon season 2012 between end of June and end of September. Before the monsoon season in early May an even higher correlation coefficient up to 0.95 was found. Correlation coefficients of 0.57-0.81 were calculated between both $\text{MLS}(\text{CO})/\text{CLaMS}(\text{CO})$ and $\text{MLS}(\text{CO})/\text{CLaMS}(\text{India/China})$ between end of June and end of September. These high correlation coefficients confirm that CLaMS has the capability of simulating the spatial distribution of tropospheric trace gases such as CO and stratospheric trace gases like O_3 measured by MLS. To illustrate this, the same horizontal cross-sections as in Figs. 2 and 3 at 380 K potential temperature for MLS CO and O_3 as well as for CLaMS CO and O_3 are shown in the Supplement of this paper.

Thus, high contributions of the emission tracers for India/China are simulated in regions where high values of CO are measured indicating that the emission tracer for India/China is a good proxy for the spatial distribution of tropospheric trace gases measured in the region of the Asian monsoon anticyclone. The correlation coefficient of $\text{MLS}(\text{CO})/\text{CLaMS}(\text{India/China})$ increases from 0. to ≈ 0.8 during the formation of the Asian monsoon anticyclone, as expected because in the model the tracer has first to be transported from the ground to the UTLS. After the breakup of the monsoon anticyclone the correlation coefficient of $\text{MLS}(\text{CO})/\text{CLaMS}(\text{India/China})$ decreases because further upward transport of the tracer for India/China does not occur due to the missing convection in this region and therefore the spatial CO distribution in the UTLS is dominated by other processes. In the region of the Asian monsoon anticyclone, the correlation coefficients of $\text{MLS}(\text{O}_3)/\text{CLaMS}(\text{O}_3)$ are somewhat higher than those of $\text{MLS}(\text{CO})/\text{CLaMS}(\text{CO})$. Reasons for that could be deficiencies in MLS CO data (v3) in the lower stratosphere as suggested by Hegglin and Tegtmeier (2015). ’

Figures 4 and 5 in the ACPD paper were moved to the Supplement of the paper and were replaced by the following Figure 1:

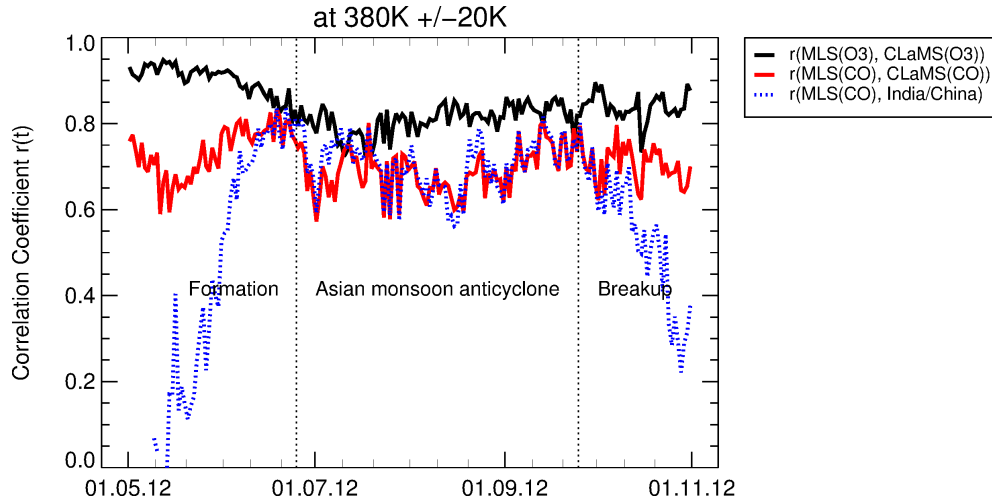


Figure 1: Correlation coefficients depending on time for tracer correlations patterns between MLS O_3 and CLaMS O_3 (black), between MLS CO and CLaMS CO (red), and between MLS CO and the CLaMS emission tracer for India/China (blue) for levels of potential temperature between 360 and 380 K (more details see text).

The section on the identification of a two-peak structure of the anticyclone (elongated or even split into two smaller ones) (discussion related to Fig. 6) is not very convincing, in my opinion. The two-peak structure searched for could easily be taken as one single broad maximum. More quantitative analysis would be needed here, should the authors decide to keep this section.

✓ We removed this section.

The section on the anticyclone tropopause as vertical transport barrier (section 3.2.2) is very important and interesting, in my opinion. The authors should consider publishing this part of the paper separately, in order not to hide it at the end of a lengthy paper.

✓ Yes, we agree that this point is very important. We follow the reviewers advice and will publish this part of the paper separately.

I recommend publication of the paper after consideration of my general remarks and specific comments as listed below.

Specific Comments

Abstract: General: The abstract is very detailed and a bit confusing. This is a pity because the paper might not get the attention it deserves. In line with my earlier general remarks, I find it would be easier and more interesting for the quick reader if the abstract was focused on fewer details; consider to boil down the abstract to few main messages of the paper.

✓ The abstract is now focused on the remaining topic of the paper after the split and should be condensed now to the main message of the paper. We revised the abstract as follows:

‘The impact of different boundary layer source regions in Asia on the chemical composition of the Asian monsoon anticyclone, considering its intraseasonal variability in 2012, is analysed by simulations of the Chemical Lagrangian Model of the Stratosphere (CLaMS) using artificial emission tracers. The horizontal distribution of simulated CO, O₃ and artificial emission tracers for India/China are in good agreement with patterns found in satellite measurements of O₃ and CO by the Aura Microwave Limb Sounder (MLS). Using in addition, correlations of artificial emission tracers with potential vorticity (PV) demonstrate that the emission tracer for India/China is a very good proxy for spatial distribution of trace gases within the Asian monsoon anticyclone. The Asian monsoon anticyclone is a transport barrier for emission tracers and is highly variable in location and shape. From end-June to early-August, a northward movement of the anticyclone and during September a strong broadening of the spatial distribution of the emission tracer for India/China towards the tropics is found. In addition to the change of the location of the anticyclone, the contribution of different boundary source regions to the Asian monsoon anticyclone strongly depends on its intraseasonal variability and is therefore more complex than hitherto believed. The largest contributions are found from North India and Southeast Asia at 380 K. In the early (mid-June to mid-July) and late (September) period of the monsoon season 2012, contributions of emissions from Southeast Asia are highest and

in the intervening period (early-August) emissions from North India have the largest impact. Our findings show that the temporal variation of the contribution different convective regions is memorised in the chemical composition of the Asian monsoon anticyclone.

Air masses originating in Southeast Asia are found both within and outside of the Asian monsoon anticyclone because these air masses experience in addition to transport within the anticyclone upward transport at the southeastern flank of the anticyclone and in the tropics and can be entrained by the outer circulation of the anticyclone. Subsequently isentropic poleward transport of these air masses occurs at around 380 K with the result that the extratropical lowermost stratosphere is flooded by end of September with air masses originating in Southeast Asia. After the breakup of the anticyclonic circulation (\approx end-September), significant contributions of air masses originating in India/China are still found in the upper troposphere over Asia. Our results demonstrate that emissions from India, China and Southeast Asia have a significant impact on the chemical composition of the lowermost stratosphere of the Northern Hemisphere in particular at the end of the monsoon season in September/October 2012. ’

Page 9942: Lines 9-11: Isn't this obvious when the anticyclone is split into two smaller ones? I'd remove this sentence.

✓ The statement is removed.

Lines 14-19: This is maybe too much detail; consider removing this sentence.

We revised the following sentence:

‘The contribution of different boundary source regions to the Asian monsoon anticyclone strongly depends on its intraseasonal variability and is therefore more complex than hitherto believed, but in general the highest contributions are from North India and Southeast Asia at 380 K.’

as follows:

‘The contribution of different boundary source regions to the Asian monsoon anticyclone strongly depends on its intraseasonal variability and is therefore more complex than hitherto believed. The highest contributions to the com-

position of the air mass in the anticyclone are found from North India and Southeast Asia at 380 K.’

Introduction: Page 9943: Lines 19-21: Really? Later you show that the tropopause above the anticyclone is an effective transport barrier; at least you should state here if this pathway is direct uplift or by isentropic poleward transport. Or maybe just change this sentence to: ‘. . . The Asian monsoon circulation IS BELIEVED to provide . . .’

✓ The statement is revised as follows:

’In general, the Asian monsoon circulation is believed to provide an effective pathway for water vapour and pollutants to the lower stratosphere of the Northern Hemisphere.’

Page 9944: Line 20-23: Is this in contradiction to your own findings?

✓ The following sentence

’In addition to the impact on the contribution of the Asian monsoon anticyclone, deep convection at the eastern/southeastern side of the Asian monsoon anticyclone can directly transport tropospheric air into the lower stratosphere by direct convective injection (Rosenlof et al., 1997; Park et al., 2007, 2008; Chen et al., 2012).’

is revised as follows:

’In addition to the impact on the contribution of the Asian monsoon anticyclone, deep convection at the eastern/southeastern side of the Asian monsoon anticyclone is discussed as a pathway for transport of tropospheric air directly into the lower stratosphere by direct convective injection (Rosenlof et al., 1997; Park et al., 2007, 2008; Chen et al., 2012).’

Page 9951: Line 3-5: ‘. . . two peaks . . . are simultaneously found forming . . . a double peak structure’. This is a redundant statement.

✓ This section is removed in the revised version of the paper.

Line 12-18: These statements here are a somewhat speculative hypothesis, and this would be fine if further elaborated and proved in the paper. Without further proven evidence, however, these statements remain speculative and should be removed.

✓ This section is removed in the revised version of the paper.

Page 9952: Line 19: What is shown from MLS is not the same as from the model - make clear from the beginning that you show a stratospheric tracer, namely ozone, and a tropospheric tracer, namely CO.

Line 23/24: ‘. . . i.e. low ozone corresponds to high percentages of the emission tracers for India/China and vice versa.’ This sentence is confusing. What you mean is low ozone = tropospheric air masses in contrast to high ozone = stratospheric air masses. However, polluted tropospheric air is expected to be higher in ozone than clean tropospheric air (still lower in ozone than stratospheric air, though). These relationships need to be clarified, otherwise it is hard to understand why polluted air loaded with emissions should come along with low ozone abundances.

✓ This section is completely revised (see above, General Remarks).

page 9953: Lines 26 ff: I find the discussion in this section not very convincing; in particular, the lower panels of Fig.6 are interpreted as giving evidence to the bi-modal distribution. For me, I must admit, it looks merely like a broad maximum distributed over the entire longitude range. There is no evidence provided that the minimum between the ‘two maxima’ is indeed significant. For me, the only obvious and convincing feature in Fig. 6 is the shift of the tracer distributions towards the South from July/August to September/October. To prove the significance of the double peak, a statistical analysis needs to be performed. E.g. one could count the days over a larger number of periods and then assign uncertainties to the numbers; a gap between the two peaks then would be significant if the difference between the peak values and the minimum in-between is larger than 2 sigma; or any other reasonable measure.

✓ We removed this Section in the revised version of the paper.

Page 9958: Lines 24 - page 9959, line 8: This justification why the 4.5 PVU

isoline can be used as boundary of the Asian monsoon anticyclone should come much earlier, e.g. page 9950, after line 9.

✓ The following sentence is added on page 9950 line 9:

' A value of 4.5 PVU is used which is in agreement with the upper limit of the PV values derived by Ploeger et al. (ACPD, 2015) to mark the transport barrier for the Asian monsoon anticyclone 2012 at 380 K.'

Pages 9959-9961, discussion of Fig. 8: How are the variations of the contributions from various source regions related to the variations of emissions from these source regions? Have the emissions assumed to be constant over time? This should then be mentioned here. In reality, emissions strengths may also have a variation over the year, thus complicating the situation.

To explain this in more detail and added the following paragraphs to the revised version of the paper:

in Sect. 2.1.1 Model Description / Emission tracers:

'The artificial emission tracers in CLaMS are designed to identify possible boundary source regions in Asia that could contribute to the composition of the Asian monsoon anticyclone in a particular monsoon season, here as a case study for the year 2012. At each time step of the model (every 24 hours) air masses in the model boundary layer are marked by the different emission tracers, i. e. the emission tracer for North India (NIN) of an air parcel in the boundary layer over Northern India is set equal to one ($NIN = 1$). If an air parcel has left the model boundary layer over North India, the value of the emission tracer for NIN ($=1$) is transported to other regions of the free troposphere or stratosphere. Successive mixing processes between air masses from North India with air masses originating in other regions of the atmosphere (here $NIN = 0$) during the course of the simulation yield values of NIN differing from the initial distribution ($NIN = 1$ or $NIN = 0$). Therefore, the value of the individual emission tracer count the percentage of an air masses that originated in the specific boundary layer region since 1 May 2012 considering advection and mixing processes.'

in Sect. 3.2.1 Temporal evolution of different emission tracer:

‘The artificial emission tracers in CLaMS are designed to identify possible boundary source regions in Asia that could contribute to the composition of the Asian monsoon anticyclone during the monsoon season 2012 (as defined in Sect. 2.1) considering advection and mixing processes. E.g. the fact that the contribution of the emission tracer for Southeast Asia dominates in June demonstrates that in June upward transport or convection in the region of Southeast Asia is stronger than in other regions over Asia causing higher contributions of the emission tracer of Southeast Asia within the Asian monsoon anticyclone compared to other emission tracers in June. By this technique contributions of the boundary layer with a transport time from the boundary to the UTLS longer than one monsoon period (contributions from the boundary layer that are released before 1 May 2012) are not covered by the artificial tracers used here. Therefore, the composition of different emission tracers within the Asian monsoon anticyclone is a fingerprint of the regional and temporal variations of convective processes causing strong upward transport within the Asian monsoon anticyclone in summer 2012.

The sum of all emission tracers shown in Fig. 8 (ACPD vers.) is less than 100 % because air masses originating in the free troposphere or stratosphere also contribute to the composition of Asian monsoon anticyclone. End of June, a contribution of 35 % of the model boundary layer to the composition of the Asian monsoon anticyclone is calculated (see here Fig. 2). The remaining 65 % of the composition of the anticyclone is from the free troposphere and the stratosphere. The contribution of the model boundary layer rises to 55 % in early August and to 75 % at the end of the monsoon season in late September.’

Page 9964, section 3.2.2: I was particularly impressed by this analysis demonstrating that the Asian monsoon anticyclone tropopause acts as a vertical transport barrier, and personally I find this is a very important result that should not be hidden at the end of a lengthy paper. I'd really encourage the authors to split the paper and to make a separate short paper out of this. When discussing the results against previous literature, the paper by Randel et al., Science, 2010 must not be ignored.

We agree that this is a very important result. Many thanks for encouraging us to highlight this in an separate short paper. That is what we will do.

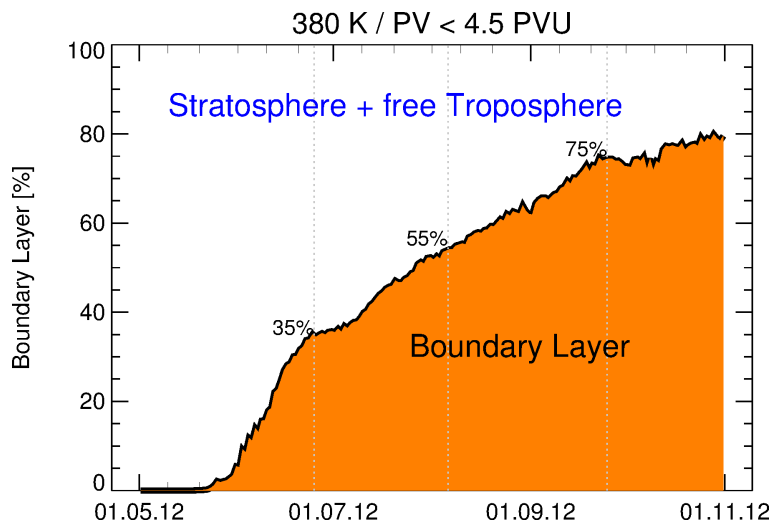


Figure 2: Temporal evolution of contributions of air masses from the boundary layer to the composition of the Asian monsoon anticyclone. The shown percentages are mean values calculated for air masses in Asia in the region between 15 and 50 N and 0 and 140 E at 380 ± 0.5 K (see black box in Fig. 1) with PV values lower than 4.5 PVU that marks the edge of the anticyclone.

Technical Comments

Page 9942, Abstract: Line 26: typo ‘still’

✓ done

Page 9943: Line 26: ‘. . . water vapour HAS a . . .’

✓ done

Page 9945: Line 23 and 26: typo : ‘source regions’ (without s)

✓ done

Page 9964: Line 6: Correct the sentence: ‘. . .are uplifted in the tropics are widely distributed . . .’

✓ This section is removed in the revised version.

Line 13: Remove one ‘the’: ‘. . . air masses from the the Asian monsoon . . .’

✓ This section is removed in the revised version.

References

Chen, B., Xu, X. D., Yang, S., and Zhao, T. L.: Climatological perspectives of air transport from atmospheric boundary layer to tropopause layer over Asian monsoon regions during boreal summer inferred from Lagrangian approach, *Atmos. Chem. Phys.*, pp. 5827–5839, doi:10.5194/acp-12-5827, 2012.

Hegglin, M. I., and Tegtmeier, S. (Eds.): SPARC Data Initiative: Assessment of Stratospheric Trace Gas and Aerosol Climatologies from Satellite Limb Sounders, SPARC Report No. 7, in preparation, 2015.

- Livesey, N. J., Filipiak, M. J., Froidevaux, L., Read, W. G., Lambert, A., Santee, M. L., Jiang, J. H., Pumphrey, H. C., Waters, J. W., Cofield, R. E., Cuddy, D. T., Daffer, W. H., Drouin, B. J., Fuller, R. A., Jarnot, R. F., Jiang, Y. B., Knosp, B. W., Li, Q. B., Perun, V. S., Schwartz, M. J., Snyder, W. V., Stek, P. C., Thurstans, R. P., Wagner, P. A., Avery, M., Browell, E. V., Cammas, J.-P., Christensen, L. E., Diskin, G. S., Gao, R.-S., Jost, H.-J., Loewenstein, M., Lopez, J. D., Nedelec, P., Osterman, G. B., Sachse, G. W., and Webster, C. R.: Validation of Aura Microwave Limb Sounder O₃ and CO observations in the upper troposphere and lower stratosphere, *J. Geophys. Res.*, 113, D15S02, doi:10.1029/2007JD008805, 2008.
- Park, M., Randel, W. J., Gettleman, A., Massie, S. T., and Jiang, J. H.: Transport above the Asian summer monsoon anticyclone inferred from Aura Microwave Limb Sounder tracers, *J. Geophys. Res.*, 112, D16309, doi:10.1029/2006JD008294, 2007.
- Park, M., Randel, W. J., Emmons, L. K., Bernath, P. F., Walker, K. A., and Boone, C. D.: Chemical isolation in the Asian monsoon anticyclone observed in Atmospheric Chemistry Experiment (ACE-FTS) data, *Atmos. Chem. Phys.*, 8, 757–764, 2008.
- Rosenlof, K. H., Tuck, A. F., Kelly, K. K., Russell III, J. M., and McCormick, M. P.: Hemispheric asymmetries in the water vapor and inferences about transport in the lower stratosphere, *J. Geophys. Res.*, 102, 13 213–13 234, 1997.

Impact of different Asian source regions on the composition of the Asian monsoon anticyclone and on the extratropical lowermost stratosphere

B. Vogel, G. Günther, R. Müller, J.-U. Grooß, and M. Riese

Forschungszentrum Jülich, Institute of Energy and Climate Research – Stratosphere (IEK-7),
Jülich, Germany

Correspondence to: B. Vogel (b.vogel@fz-juelich.de)

Abstract

The impact of different boundary layer source regions in Asia on the chemical composition of the Asian monsoon anticyclone, considering its intraseasonal variability in 2012, is analysed by ~~CLaMS simulations using artificial emission tracers. Our simulations show that the Asian monsoon anticyclone is highly variable in location and shape and oscillates between 2 states: first a symmetric anticyclone and second, an asymmetric anticyclone either elongated or split in two smaller anticyclones. A maximum in the distribution of air originating from Indian/Chinese boundary layer sources is usually found in the core of the symmetric anticyclone, in contrast the asymmetric state is characterised by a double peak structure in the horizontal distribution of air originating from India and China. The simulated simulations of the Chemical Lagrangian Model of the Stratosphere (CLaMS) using artificial emission tracers. The horizontal distribution of simulated CO, O₃ and artificial emission tracers for India/China is in are in good agreement with patterns found in satellite measurements of O₃ and CO by the Aura Microwave Limb Sounder (MLS). The Using in addition, correlations of artificial emission tracers with potential vorticity (PV) demonstrates that the emission tracer for India/China is a very good proxy for spatial distribution of trace gases within the Asian monsoon anticyclone. The Asian monsoon anticyclone constitutes a horizontal transport barrier for emission tracers and is highly variable in location and shape. From end-June to early-August, a northward movement of the anticyclone and during September, a strong broadening of the spatial distribution of the emission tracer for India/China towards the tropics is found. In addition to the change of the location of the anticyclone, the contribution of different boundary source regions to the Asian monsoon anticyclone strongly depends on its intraseasonal variability and is therefore more complex than hitherto believed, but in general the highest contributions are. The largest contributions to the composition of the air mass in the anticyclone are found from North India and South-east Asia at a potential temperature of 380 K. In the early (June mid-June to mid-July) and late (mid-August to October September) period of the monsoon season 2012, contributions of emissions from Southeast Asia are highest and in the intervening period (≈mid-July to~~

mid-August/early-August) emissions from North India have the largest impact. Further, our simulations confirm that the thermal tropopause above the anticyclone constitutes a vertical transport barrier. Enhanced contributions of emission tracers for Asia are found at the northern flank. Our findings show that the temporal variation of the contribution of different convective regions is memorised in the chemical composition of the Asian monsoon anticyclone between double tropopauses indicating an isentropic transport from the anticyclone into the lowermost stratosphere.

After the breakup of the anticyclone, significant contributions of air masses originating in India/China are still found over Asia in September/October. In addition, Southeast Asia are found both within and outside of the Asian monsoon anticyclone because these air masses spread out within the mid-latitudes of the Northern Hemisphere experience in addition to transport within the anticyclone upward transport at the southeastern flank of the anticyclone and in the tropics at around 380. Moreover, air masses from Southeast Asia experienced diabatic upward transport in the tropics and subsequently and can be entrained by the outer circulation of the anticyclone. Subsequently isentropic poleward transport of these air masses occurs at around 380 K with the result that the extratropical lowermost stratosphere in the Northern Hemisphere is flooded by end of September with air masses originating in Southeast Asia. Even after the breakup of the anticyclonic circulation (\approx end-September), significant contributions of air masses originating in India/China are still found in the upper troposphere over Asia. Our results demonstrate that emissions from India, China and Southeast Asia have a significant impact on the chemical compositions of the lowermost stratosphere of the Northern Hemisphere in particular after at the end of the monsoon season in September/October 2012.

1 Introduction

The Asian summer monsoon circulation is an important global circulation system in northern summer associated with strong upward transport of tropospheric source gases into the upper troposphere and lower stratosphere (UTLS) region (e.g. Li et al., 2005; Randel

and Park, 2006; Park et al., 2007, 2008, 2009). Satellite measurements show that tropospheric trace gases such as water vapour (H₂O), carbon monoxide (CO), nitrogen oxides (NO_x), Peroxyacetyl nitrate (PAN), hydrogen cyanide (HCN), and aerosol are confined by the strong anticyclonic circulation in the UTLS and therefore are isolated from the surrounding air (Rosenlof et al., 1997; Jackson et al., 1998; Park et al., 2004, 2008; Li et al., 2005; Xiong et al., 2009; Randel et al., 2010; Vernier et al., 2011; Bourassa et al., 2012; Fadnavis et al., 2013, 2014). In contrast, stratospheric trace gases such as O₃, HNO₃, or HCl show low concentrations in the anticyclone (Randel and Park, 2006; Park et al., 2008; Liu et al., 2009; Konopka et al., 2010). In general, the Asian monsoon circulation provides is believed to provide an effective pathway for water vapour and pollutants to the lower stratosphere of the Northern Hemisphere (Bian et al., 2012; Ploeger et al., 2013; Vogel et al., 2014; Uma et al., 2014). ~~However, the mechanisms for~~ The mechanisms for possible transport into the lowermost stratosphere are subject of a longstanding debate (Dethof et al., 1999; Park et al., 2009; Randel et al., 2010; Bourassa et al., 2012; Fairlie et al., 2014; Fromm et al., 2014; Vogel et al., 2014).

Increasing stratospheric water vapour have has a significant influence on the climate system (e.g. Forster and Shine, 1999; Shindell, 2001; Smith et al., 2001; Forster and Shine, 2002; Vogel et al., 2012), in particular the variability of water vapour in the lower stratosphere is an important driver of surface climate change (e.g. Solomon et al., 2010; Riese et al., 2012). In addition, increasing stratospheric water vapour plays a crucial role in stratospheric chemistry (e.g. Kirk-Davidoff et al., 1999; Dvortsov and Solomon, 2001; Vogel et al., 2011a). Therefore, it is important to understand transport processes from the Asian monsoon region into the global lower stratosphere.

Moreover, the contribution of different boundary source regions in Asia to the chemical composition of the Asian monsoon anticyclone (e.g. Li et al., 2005; Park et al., 2009; Chen et al., 2012; Bergman et al., 2013; Fadnavis et al., 2014) is currently discussed. Chen et al. (2012) found that most impact at tropopause heights is from emissions originating in the tropical Western Pacific region and the South China Sea, while Bergman et al. (2013) found that air masses originating at the Tibetan Plateau and in India are most important at

100 hPa. Simulations with a chemistry transport model by Park et al. (2009) show that the main surface sources of CO in the Asian monsoon anticyclone are from India and Southeast Asia, whereby the weak contribution of air masses originating from the Tibetan plateau in their analysis is due to the lack of significant surface emissions of CO in this region [in their model simulations](#). Further, air masses from northeast India and southwest China uplifted at the eastern side of the anticyclone could also contribute to the chemical composition of the Asian monsoon anticyclone (Li et al., 2005).

In addition to the impact on the contribution of the Asian monsoon anticyclone, deep convection at the eastern/southeastern side of the Asian monsoon anticyclone ~~can directly transport tropospheric air~~ [is discussed as a pathway for transport of tropospheric air directly](#) into the lower stratosphere by direct convective injection (Rosenlof et al., 1997; Park et al., 2007, 2008; Chen et al., 2012). However, the impact of this transport mechanism on the chemical composition of the lower stratosphere has not been isolated from the exchange between the troposphere and the stratosphere associated with the large-scale Brewer–Dobson circulation (Gettelman et al., 2004; Bannister et al., 2004).

The monsoon and the associated seasonal change of wind and rainfall is characterised by prolonged periods of dry and wet conditions in the range of 2–3 weeks. Extended periods with enhanced precipitation (wet spells) characterise active conditions, while dry spells represent periods when a break in monsoon activity occurs (Goswami, 2012, and references therein). The active and break phases are manifestations of the superposition of large scale northward moving 30 to 60 day oscillations and small scale westward propagating 10 to 20 day variations, however ~~the detailed understanding of the variability is an open question~~ [details of this variability are far from being well understood](#) (Goswami, 2012, and references therein). This intraseasonal variability of the monsoon is associated with the strength of the Asian monsoon anticyclone in the UTLS (Goswami, 2012). ~~Therefore~~ [Further](#), the evolution over the monsoon season of the anticyclone is characterised by large variability in its extent, strength and location (e.g. Randel and Park, 2006). Garny and Randel (2013) found that the temporal variability of the strength of the anticyclone, as diagnosed by

low areas of potential vorticity (PV), is driven by the variability in convection with a period of 30–40 days.

~~Further, westward transport of low PV values or smaller anticyclones separated from the Asian monsoon anticyclone (referred to as “eddy shedding”) occurs more often than the process of eastward migrating smaller anticyclones during the monsoon season (Garny and Randel, 2013). Moreover, also~~ Also splittings of the Asian monsoon anticyclone into two separate smaller anticyclones frequently occur each year (e.g. Garny and Randel, 2013). ~~They report that the longitudinal location of the core of the Asian monsoon anticyclone has two preferred regions, referred to as Tibetan Mode and Iranian Mode, affecting the distribution of chemical constituents in the UTLS (?).~~

In this paper, we investigate what the following main questions. What is the impact of different boundary layer ~~sources~~ source regions in Asia on the composition of air in the Asian monsoon anticyclone 2012 considering the intraseasonal variability of the anticyclone. ~~?~~ Further, we analyse how both boundary layer ~~sources~~ source regions in Asia and the Asian monsoon anticyclone affect the chemical composition of the lowermost stratosphere ~~for the example of the year 2012.~~

The summer 2012 is a good example for normal monsoon conditions. The rainfall in India was normal based on the rainfall data set of 306 rain gauges in India provided by the Indian Institute of Tropical Meteorology in Pune, India¹. A strong relation between rainfall (droughts or floods) during the Indian summer monsoon to El Niño and La Niña events have been established (e. g. Webster et al., 1998; Kumar et al., 2006). In summer 2012 neutral conditions for the El Niño/Southern Oscillation (ENSO) occurred according to the Oceanic Niño Index (ONI)².

To answer ~~these questions, we perform our question, we performed~~ simulations with the three-dimensional Lagrangian chemistry transport model (CLaMS) (McKenna et al., 2002b, a; Konopka et al., 2012, and references therein). ~~CLaMS results are compared with measurements from the Aura Microwave Limb Sounder (MLS).~~ The paper is organ-

¹see e.g., <http://www.tropmet.res.in/~kolli/mol/Monsoon/Historical/air.html>

²see e.g., <http://ggweather.com/enso/oni.htm>

ised as follows: Sect. 2 describes the CLaMS simulations ~~using artificial tracers and the use of inert artificial tracers of air mass origin to mark boundary layer source regions~~. In Sect. 3, ~~the evolution of the Asian monsoon anticyclone is described and CLaMS results are presented and compared to MLS measurements~~ ~~— compared with measurements from the Aura Microwave Limb Sounder (MLS)~~. ~~Further, the impact of different emission tracers to the composition of the anticyclone is calculated for the entire monsoon season 2012~~. The conclusions are given in Sect. 4.

2 The Chemical Lagrangian Model of the Stratosphere (CLaMS)

2.1 Model description

Model simulations were performed using the Chemical Lagrangian Model of the Stratosphere (CLaMS), a three-dimensional chemistry transport model that was originally developed for the stratosphere (e.g. McKenna et al., 2002b, a; Grooß et al., 2005; Grooß and Müller, 2007) and extended to the troposphere (Konopka et al., 2010, 2012; Pommrich et al., 2014, and references therein). It was shown in previous studies, that CLaMS is very well-suited to simulate strong tracer gradients of chemical species in regions where transport barriers exist like the polar vortex (e.g. Günther et al., 2008; Vogel et al., 2008), the extra-tropical tropopause and in the vicinity of the jet streams (e.g. Pan et al., 2006; Konopka et al., 2010; Vogel et al., 2011b; Konopka and Pan, 2012).

CLaMS is based on a Lagrangian formulation of tracer transport and considers an ensemble of air parcels on a time-dependent irregular grid that is transported by use of 3-D-trajectories. The irreversible part of transport, i.e. mixing, is controlled by the local horizontal strain and vertical shear rates with mixing parameters deduced from observations (Konopka et al., 2010, and references therein). Here, we present results of global CLaMS simulations that cover an altitude range from the surface up to 900 K potential temperature (≈ 37 km altitude) with a horizontal resolution of 100 km and a maximum vertical resolution of approximately 400 m at the tropopause. The horizontal winds are taken from the ERA-Interim

reanalysis (Dee et al., 2011) provided by the European Centre for Medium-Range Weather Forecasts (ECMWF). [Changes in this data set, changes](#) are implemented to improve deep and mid-level convection in ERA-Interim data in contrast to previous reanalysis data (Dee et al., 2011).

Mixing parameter, vertical coordinate, and the cross-isentropic velocity of the model follow the model set-up described by Konopka et al. (2012). Convection in CLaMS is represented by vertical velocities in ERA-Interim reanalysis data. CLaMS employs a hybrid coordinate (ζ), which transforms from a strictly isentropic coordinate Θ to a pressure-based coordinate system (more details see Pommrich et al., 2014).

For this study, the CLaMS simulation includes full stratospheric chemistry (Groß et al., 2014; Sander et al., 2011) and was initialised on 1 May 2012 based on data from AURA-MLS version 3.3 (Livesey et al., 2011) and ACE-FTS version 3.0 and on results of a multi-annual CLaMS simulation started on 1 October 2001 (Konopka et al., 2010). Global O_3 , CO , H_2O , HCl , and N_2O fields are derived from MLS data within ± 2.5 days, while the trajectory-determined synoptic locations have been composed to a $2^\circ \times 6^\circ$ (latitude-longitude) grid. Below $\zeta = 350$ K (equal to $\Theta = 350$ K), these species were taken from the CLaMS multi-annual simulation with a linear transition between $\zeta = 350$ and 400 K (equal to $\Theta = 350$ – 400 K). CO_2 is initialised from this simulation within the whole vertical domain.

The initialisation of CH_4 , NO_y , CFC-11, and CFC-12 was derived from N_2O using correlation fits for different latitude bins derived from ACE-FTS version 3.0 data between April and August 2010 following Groß et al. (2014). The remaining species and the initial partitioning of the chemical families were taken from correlations and the Mainz 2-D model as described by Groß et al. (2014). At the upper boundary (900 K potential temperature) AURA-MLS and ACE-FTS measurements and tracer-tracer correlations were used similarly as for the initialisation besides CO which was taken from MLS V3.3 data.

At the lower boundary (surface), O_3 is set to a constant tropospheric value of 4.8×10^{-8} volume mixing ratio representing the ozone mixing ratio at 5 km (Brasseur and Solomon, 2005, p. 619). Water vapour is replaced by ECMWF water vapour in lower model levels. Lower boundary conditions for CO and CH_4 are derived from AIRS (Atmospheric Infrared

Sounder) satellite measurements version 6 following the approach described by Pommrich et al. (2014).

2.1.1 Emission tracers

The aim of our study is to analyse transport pathways of air masses from boundary layer sources to the Asian monsoon anticyclone and further the transport of these air masses into the extratropical lowermost stratosphere. Three-dimensional CLaMS simulations were performed to include both the advective transport and the irreversible part of transport, namely mixing. The use of artificial tracers in CLaMS that mark particular regions in the atmosphere allows to quantify the origin of air masses, the pathways, and the transport times to be quantified (Günther et al., 2008; Vogel et al., 2011a).

Here, inert artificial tracers of air mass origin, hereafter referred to as “emission tracers”, are introduced that mark globally all land masses in the Earth’s boundary layer ($\approx 2\text{--}3$ km above surface following orography corresponding to $\zeta < 120$ K) and thus represent regionally different boundary layer sources regions. Figure 1 shows the geographic **regions** **locations** defined for all 13 emission tracers (red boxes). The latitude and longitude range of each box that represents one emission tracer is listed in Table 1. ~~Regions in the boundary layer not considered in~~ Further, the remaining tropical regions (20° S – 20° N) over the oceans are also marked by artificial tracers (TPO = Tropical Pacific Ocean, TAO = Tropical Atlantic Ocean, TIO = Tropical Indian Ocean) as indicated by blue lines in Fig. 1. Boundary layer regions not considered by the defined emissions tracers listed in Table 1 are summarised in an emission tracer for the background. Because we are in particular interested in the contributions of different boundary layer source regions in Asia to the composition of air within the Asian monsoon anticyclone, the regions defining emission source regions in Asia are ~~chosen smaller~~ better resolved than in regions elsewhere. The separation in different regions in Asia is chosen to separate regions that are currently discussed in the literature as possible source regions (see Sect. 1). The most important regions for our study are North India (NIN), South India (SIN), East China (ECH), and Southeast Asia (SEA). To discuss the CLaMS results, the percentages of emission tracers for North India (NIN),

South India (SIN) and East China (ECH) are sometimes summarised in one emission tracer referred to as “India/China” (India/China = NIN + SIN + ECH).

The artificial emission tracers in CLaMS are designed to identify possible boundary source regions in Asia that could contribute to the composition of the Asian monsoon anticyclone in a particular monsoon season, here as a case study for the year 2012. At each time step of the model (every 24 hours) air masses in the model boundary layer are marked by the different emission tracers, i. e. the emission tracer for North India (NIN) of an air parcel in the boundary layer over Northern India is set equal to one (NIN = 1). If an air parcel has left the model boundary layer over North India, the value of the emission tracer for NIN (=1) is transported as like a chemical tracer to other regions of the free troposphere or stratosphere. Successive mixing processes between air masses from North India with air masses originating in other regions of the atmosphere (here NIN= 0) during the course of the simulation yield values of NIN differing from the initial distribution (NIN = 1 or NIN = 0). Therefore, the value of the individual emission tracer counts the percentage of an air masses that originated in the specific boundary layer region since 1 May 2012 considering advection and mixing processes.

3 Results

3.1 **The Evolution of Asian monsoon anticyclone 2012**

3.1.1 **Spatio-temporal evolution of the Asian monsoon anticyclone 2012**

The spatio-temporal evolution of the Asian monsoon anticyclone in summer 2012 is inferred from three-dimensional CLaMS simulations using the abovementioned emission tracers for Asia. The CLaMS simulation starts on 1 May 2012 before the formation of the Asian monsoon anticyclone begins during June and ends late October after the breakup of the anticyclone. Deep convection (represented in CLaMS by vertical velocities in ERA-Interim reanalysis data; see Sect. 2.1) leads to strong upward transport of emission tracers from

source regions in Asia within the Asian monsoon anticyclone. Our simulation confirms that the extent, strength, and location of the anticyclone is highly variable (e.g. Annamalai and Slingo, 2001; Randel and Park, 2006; Garny and Randel, 2013). In particular, the ~~locations of peaks with maximum contributions of emission tracers for India/China~~ location and the shape of the anticyclone change from day to day which is demonstrated in the following.

Because the Asian monsoon anticyclone is characterised by low PV, the horizontal distributions of the emission tracer for India/China in comparison to the horizontal distribution of PV is analysed at 380 K potential temperature (≈ 16 km) (see Figs. 2 and 3). The level of 380 K potential temperature is located within the Asian monsoon anticyclone just below the thermal tropopause (~~see Sect. ??~~). To discuss the spatio-temporal evolution of the Asian monsoon anticyclone, 6 days are selected reflecting typical situations of the evolution of the Asian monsoon anticyclone. The 1 July 2012 shows conditions at the beginning of the evolution of the Asian monsoon (early-phase), here the anticyclone is centred over Tibet. The 28 July, 2 August and 8 August 2012 are days in the ~~middle-period~~ mid-phase of the monsoon season, here a strong asymmetric anticyclone, a symmetric anticyclone centred over Iran and an anticyclone split into two smaller anticyclones are found. ~~At the end of the monsoon period on 20~~ On 12 September 2012, ~~the separation of a large eastward migrating weaker anticyclone (eddy shedding event) of the main anticyclone is found.~~ Finally, the ~~19~~ conditions during the late-phase of the monsoon and on 7 October 2012 ~~was selected to show the horizontal distribution of emission tracers for India/China~~ the situation after the breakup of the anticyclone occurring end-September are shown.

On 1 July 2012 (Fig. 2, top), the anticyclone is centred over Tibet. The northern flank of the anticyclone border on the subtropical westerly jet and the southern flank to the equatorial easterly jet. In our study, the region of strongest gradients in the horizontal distribution of emission tracers from Asia represent the edge of the anticyclone at 380 K. A ~~fixed-PV value of about~~ value of 4.5 PVU (thick white line) is introduced ~~in Fig. 2 to mark regions with low PV (< 4.5)~~ which is in agreement with the upper limit of the PV values derived by Ploeger et al. (2015) to mark the transport barrier for the Asian monsoon anticyclone 2012 at 380 PVU (more details see Sect. 3.2.1). Filaments consisting of air masses charac-

Discussion Paper | Discussion Paper | Discussion Paper

terised by low PV values (< 4.5 PVU) and enhanced emissions from India/China occur both at the western and eastern flank of the anticyclone.

On 28 July 2012 (Fig. 2, 2nd row), the horizontal distribution of high percentages of emission tracers for India/China shows an elongated structure with maxima at its two endpoints located over Northeast Africa and Southeast China (red coloured). ~~Similar patterns are found for the absolute vorticity in theoretical calculations by ? to investigate nonaxisymmetric thermally driven circulations within the monsoon dynamic.~~ The shape of the PV isoline of 4.5 PVU includes two anticyclones situated close together.

After 28 July 2012, the western peak is transported eastwards and the eastern peak moves westwards and both peaks merge in one location in early August. On 2 August 2012 (see Fig. 2, 3rd row), the anticyclone again has a more symmetric shape and is centred over Iran and Afghanistan. The spatial distribution of emission tracers for India/China shows two regions with maximum values one in the core of the anticyclone over Iran and Afghanistan and another smaller within the anticyclone farther northeast over China. This pattern is a remnant of the elongated structure found in the distribution of emission tracers for India/China on 28 July 2012 caused by the double peak structure of the Asian monsoon anticyclone. This small-scale structure found in the horizontal distribution of emission tracers for India/China is also evident in the spatial distribution of low PV values. On 8 August 2012 (see Fig. 2, bottom), the Asian monsoon anticyclone is split into two smaller anticyclones, one centred over the northern Middle East (Iraq/Iran) and a second one over East China.

~~These examples show that at some days, two peaks with enhanced percentages of the emission tracers for India/China are simultaneously found at different locations at 380, forming a double peak structure. The locations of the two peaks differ in east-west direction and sometimes in addition in north-south direction. The two peaks can be completely separated, manifested in two smaller anticyclones, or they are endpoints of elongated stretched structures appearing as a strongly asymmetric anticyclone. In our simulation, such pronounced double peak structure in the spatial distribution of the emission tracers for India/China at 380 is found to occur on average every 10–30 (at 7 June, 18 June,~~

17 July, 28 July, 8 August, 27 August, 18 September, and 29 September 2012). Thus, looking on the horizontal distribution of emission tracers the spatial distribution of the emission tracer for India/China , the Asian monsoon anticyclone oscillates between 2 states: first, a strongly symmetric anticyclone filled in the core with air masses originating from boundary source in India/China and second, a double peak structure, a strongly asymmetric anticyclone either elongated or split in two smaller anticyclones also filled with air masses from India/China. We assume that this behaviour is caused by the intraseasonal variability of the Asian summer monsoon related to its active and break phases (e.g. Goswami, 2012, and references therein).

Moreover, at the northeast flank of the Asian monsoon anticyclone, either filaments with enhanced contributions of emission tracers for India/China are separated from the anticyclone or eastward migrating smaller anticyclones (eddy shedding) are breaking off from the main anticyclone a few times during the summer 2012 carrying enhanced contributions of air masses from India/China further eastwards. A strong eddy shedding event occurred on 20 September 2012 is shifted towards the tropics compared to the mid-phase as shown in Fig. 3 (top). The meteorological conditions for this event are discussed in detail in Vogel et al. (2014). A smaller anticyclone located over the Pacific Ocean is separated from the main anticyclone centred over North India/Tibetan Plateau. Afterwards, the second anticyclone moves to the Pacific Ocean along the subtropical westerly jet and transports air masses with enhanced contributions from India/China within a few days (roughly 8–14) to the lowermost stratosphere over northern Europe. Therefore, in general filaments of smaller anticyclones separated at the northeast flank of the anticyclone have the capability to rapidly transport water vapour and pollutants from Asia to the lowermost stratosphere over North America and Europe (e.g. Vogel et al., 2014).

In 2012, the breakup of the Asian monsoon anticyclone occurred in late September and early October. Figure 3 (bottom) shows the spatial distribution of the emission tracers for India/China at 380 K after the breakup on 19 October 2012. The breakup of the anticyclone or the disappearance of the transport barrier goes along with the spread of the emission tracers for India/China at 380 K within the mid-latitudes of the Northern Hemisphere and

in the tropics. High percentages of the emission tracers for India/China are found over the Pacific Ocean and over the east coast of North America along the subtropical westerly jet. The subtropical jet is in addition a transport barrier for the transport further polewards into the lowermost stratosphere of air masses originating in the boundary layer in India/China. In addition, air masses originating in the boundary layer in India/China could penetrate into the upwelling in the deep branch of the Brewer–Dobson circulation and could in this way reach the upper stratosphere.

3.1.1 Comparison to MLS measurements

To compare our simulation ~~results with~~ with MLS O_3 and CO measurements ~~by MLS~~ (Version 3.3) (Livesey et al., 2008), ~~the same horizontal cross-sections as in Figs. 2 and 3 at 380 potential temperature are shown in Figs. ?? and ??.~~ In general at 380, ~~the horizontal distributions of the stratospheric tracer~~ pattern correlation coefficients between MLS measurements and CLaMS results, namely $MLS(CO)/CLaMS(CO)$, $MLS(O_3)$ ~~show very similar patterns as the spatial distribution of the emission tracers for India/China calculated in our simulation, i.e. low ozone corresponds to high percentages of the emission tracers for India~~ $CLaMS(O_3)$ and $MLS(CO)/CLaMS(India/China)$, were calculated between 360 and 400 K potential temperature (see Fig. 4). It is expected from satellite measurements that CO mixing ratios are higher within the Asian monsoon anticyclone than outside and vice versa. ~~Features like the filamentary structure on the western and eastern flank of the anticyclone on 1 July 2012, the elongated double peak structure on 28 July 2012, the symmetric structure with a westward eddy shedding on 2 August 2012, the split for O_3 indicating that air masses inside the anticyclone have a stronger tropospheric characteristic than air masses in the UTLS outside of the anticyclone into two smaller anticyclones on 8 August. At all days between 1 May 2012, the strong eastward eddy shedding event on 20 September and 31 October 2012, and the tracer distribution after the breakup of the anticyclone on 19 October 2012 are also evident in the MLS measurements.~~ In addition, in the Northern Hemisphere ~~CLaMS simulations of show the same patterns as MLS~~ MLS measurements of O_3 at 380 and CO in a region between 15 and 50° potential temperature. Figures for CLaMS

are shown in the Supplement of this paper. N and 0 and 140° E (shown as black rectangle in Fig. 2) between 360 and 400 K potential temperature are correlated to CLaMS results as described in the following. At each day, CLaMS results are interpolated on locations of the MLS measurements transformed to synoptic 12:00 UTC positions. For each day, both MLS measurements and CLaMS results are normalised so that the maximum value of each trace gas is equal one. Afterwards the linear Pearson correlation coefficient $r(t)$ between MLS measurement and CLaMS results is calculated for each day. This procedure allows the spatial distribution of trace gases to be compared neglecting possible differences in the absolute mixing ratios between model and measurement and to compare the spatial distribution of different quantities such as measured CO as a tropospheric tracer is expected to show high values in regions with high contributions of the emission tracers for and simulated emission tracers (here India/China, however the features mentioned above are less distinct in MLS than in . Reasons for that could be deficiencies in MLS).

Correlation coefficients $r(t)$ ranging between 0.72 and 0.86 were calculated for $MLS(O_3)/CLaMS(O_3)$ during the monsoon season 2012 between end of June and end of September. Before the monsoon season in early May an even higher correlation coefficient up to 0.95 was found. Correlation coefficients of 0.57 to 0.81 were calculated for both $MLS(CO\text{ data (v3) in the lower stratosphere as suggested by Hegglin and Tegtmeier (2015) })/CLaMS(CO; \text{ however due to the coarse spatial resolution of })$ and $MLS(CO\text{ and possible deficiencies in MLS })/CLaMS(\text{India/China})$ between end of June and end of September. These high correlation coefficients confirm that CLaMS has the capability of simulating the spatial distribution of tropospheric trace gases such as CO , the agreement is not quite as good as for and stratospheric trace gases like O_3 . However, the comparison between CLaMS simulations and MLS measurements shows that the model yields realistic patterns of the contribution of emission tracers in measured by MLS. In the region of the Asian monsoon anticyclone at 380-

Previous studies (??) found that the longitudinal location of the anticyclone core has two preferred regions at 100, referred to as Tibetan Mode (80–90E) and Iranian Mode (55–65E)

, impacting the spacial distribution of chemical trace gases in this region. Our simulations show that the shape of the anticyclone oscillates between a strongly symmetric anticyclone and second, a double peak structure, a strongly asymmetric anticyclone either elongated or split in two smaller anticyclones as discussed above (, the correlation coefficients of $MLS(O_3)/CLaMS(O_3)$ are somewhat higher than those of $MLS(CO)/CLaMS(CO)$. Reasons for that could be deficiencies in $MLS\ CO$ data (v3) in the lower stratosphere as suggested by Hegglin and Tegtmeier (2015). To illustrate the good agreement between $CLaMS$ and MLS , the same horizontal cross-sections as in Figs. 2 and 3). If we assume that the highest percentages of the emission tracers for India/China are found in the core region of the anticyclone, the Tibetan Mode and Iranian Mode should be also evident in the distribution of emissions tracers for India/China in the $CLaMS$ simulations as found for chemical constituents in the UTLS (?). Therefore, we calculate mean values of the contributions of emission tracers for India/China for July/August 2012 in latitude-longitude bins (of $2.5 \times \text{longitude} (\lambda) \times 1.0^\circ \text{ latitude} (\phi)$) at 380 K : potential temperature for $MLS\ CO$ and O_3 as well as for $CLaMS\ CO$ and O_3 are shown in the Supplement of this paper.

Figure ?? (left, top panel) shows the number of days ($N(\lambda, \phi)$) where in the region of the Asian monsoon anticyclone air masses are found with mean values of the contributions of emission tracers for India/China exceeding 35 for July/August 2012. The value of 35 is chosen because it considers relatively high contributions of the is simulated in regions where high values of CO are measured indicating that the emission tracer for India/China . Choosing a higher percentage would not consider lower contributions of the emission tracers for India is a very good proxy for the spatial distribution of tropospheric trace gases measured in the Asian monsoon anticyclone. The correlation coefficient of $MLS(CO)/China$ found in the core of the anticyclone in early July due to the transport times of air masses originating in boundary layer in $CLaMS$ (India/China up to the 380 level).

An accumulation of days with contributions of emission tracers for China) increases from 0 to ≈ 0.8 during the formation of the Asian monsoon anticyclone, as expected

because in the model the tracer has first to be transported from the ground to the UTLS. After the breakup of the monsoon anticyclone the correlation coefficient of $MLS(CO)/CLaMS$ (India/China larger than 35 are found over Afghanistan/Pakistan and over Nepal) decreases because further upward transport of the tracer for India/Tibet (in $\approx 1/3$ of all days in July China does not occur due to the missing convection in this region and therefore the spatial CO distribution in the UTLS is dominated by other processes.

3.1.2 Different phases of the Asian monsoon anticyclone

To link the temporal variation of the spatial distribution of the emission tracers also to areas of low PV during the entire Asian monsoon period 2012, pattern correlation between PV and the emission tracer for Indian/August) within a latitude range of 28–36° China (red), the emission tracer Southeast Asia (grey) and CLaMS CO (blue) are calculated as shown in Fig. 5. The correlation coefficients are calculated in a region between 15 and 50° N. Maximum occurrence are found in longitude intervals of approximately 60–75 and 80–90 and 0 and 140° E (see shown as black rectangle in Fig. ?? left, bottom panel). In the simulated tracer distribution, a bimodal longitudinal structure is also found, however the maxima found at 60–75° at 380 E are shifted to somewhat higher longitudes compared to the Iranian Mode (55–65° similar as for the $MLS/CLaMS$ correlations described above. For each day, CLaMS results and PV are interpolated on 1×1 latitude longitude grid at 380 E) derived by ?. Reasons could be that here the distribution of emission tracers is used in contrast to K and thereafter normalised to one.

Fig. 5 shows that the study by ? where the dynamical core of the anticyclone is derived based on considering geopotential on pressure surfaces of 100. It must be emphasised that this bimodal distribution has been seen in the dynamical structure of the anticyclone (?), found in satellite measurements (?) and in the CLaMS simulations is not simply an east-west shift spatial distribution of PV and CLaMS CO is very well correlated during the formation (-0.89 to -0.95), the existence (-0.74 to -0.93) and the breakup (-0.68 to -0.89) of the Asian monsoon anticyclone. In the course of the Asian monsoon season, a good correlation between the spatial distribution of low PV and and high percentages

of the emission tracer for India/China of -0.71 to -0.87 is found. During the formation of the anticyclone, ~~but rather~~ the correlation coefficients increases because the emission tracer has to be transported up to the UTLS. The decrease of the correlation coefficients after the breakup is caused by the ~~oscillation between strongly symmetric and asymmetric anticyclones as shown in Figs. 2 and 3 (left). Besides of the 2 maxima (modes), lower maxima are found in the longitudinal distribution (see~~ missing convection in Asia occurring during the monsoon season (see comparison between MLS and CLaMS in Sect. 3.1.1). In contrast, the correlation coefficient between the spatial distribution of PV and the emission tracer for Southeast Asia shows a completely different behaviour. During the formation of the Asian monsoon the contributions of the emission tracer for Southeast Asia increase similarly as for the emission tracer for India/China. During the existence of the anticyclone a high correlation coefficient up to -0.90 is calculated at the early- and late-phase of the anticyclone, however in early August (mid-phase) the correlation between the spatial distribution of PV and the emission tracer for Southeast Asia almost vanishes (indicated by the black dashed line in Fig. ?? left, bottom panel) at 50E reflecting the transport (5). This shows that in the mid-phase the spatial distribution of air masses from originating in Southeast Asia is not connected to region of the Asian monsoon anticyclone to the west by westward eddy shedding (or outflow) and at 100E caused by eastward eddy shedding and the release of filaments at the northeastern flank of the anticyclone (Vogel et al., 2014) indicating that air masses from Southeast Asia experienced upward transport outside of the Asian monsoon anticyclone (see Sect. 3.2).

~~The same analysis is also performed for September~~ The good correlation found between the emission tracer for India/October 2012, the end phase of the monsoon season and its breakup (Fig. ??, right). Here, the region with an accumulation of days with contributions of emission tracers China and MLS measurements as well as PV confirms that the spatial distribution of the emission tracer for India/China is a very good proxy for the location and shape of Asian monsoon anticyclone from end-June to end-September.

Figure 6 shows twelve-day mean values of the emission tracer for India/China and PV during different phases of the Asian monsoon anticyclone. A slight geographical northwards

shift of the spatial distribution of the emission tracer for India/China larger than 35 (in $\approx 1/4$ of all days in September from the early-phase of the anticyclone from end-June/October) is shifted to the tropics and broadened both to the east and to the west. This shows that also in September and October 2012 enhanced contributions of boundary emissions are found over Asia at 380, even though the confinement of the Asian monsoon anticyclone has dissipated during that time period. Also here, a bimodal distribution is found with two maxima one at 40–60E and a second at 75–110E (Fig. ?? right, bottom panel) early-July to early-August (mid-phase) is found. Further in early-September, the late-phase of the anticyclone, a much broader spatial distribution of the emission tracer for India/China is found, in particular the southern edge of the anticyclone is shifted towards the tropics. In early-October after the breakup of the anticyclone, still high percentages of the emission tracer for India/China are found over India, China and the Pacific Ocean.

Animations showing the temporal evolution (on a daily basis) of the contribution of emission tracers for India/China, Southeast Asia and PV at 380 K potential temperature on the Northern Hemisphere during the Asian monsoon season 2012 (1 May 2012–late October 2012) are available as a Supplement of this paper showing the intraseasonal variability of the Asian monsoon anticyclone. In the next [section sections](#), the spatial distribution of different emission tracers for Asia within the Asian monsoon anticyclone and the temporal evolution of all tracers within the Asian monsoon anticyclone from May until late October 2012 are discussed.

3.1.3 Impact of different emission tracers to the composition of the Asian monsoon anticyclone

3.2 Impact of different emission tracers to the composition of the Asian monsoon anticyclone

To analyse the possible impact of different boundary layer source regions in Asia, in particular the specific importance of Southeast Asia, to the composition of the Asian monsoon anticyclone, the horizontal distributions of emission tracers are discussed at 380 K potential

temperature using the four days introduced in the previous section (1 July, 2 and 8 August, and 2012 September 2012, see Sect. 3.1.1). The emission tracers for North India, South India, and East China show in principle the same horizontal patterns, therefore here we show only emissions from North India. However, their individual contributions to the composition of the anticyclone differ from tracer to tracer and are time dependent (see Sect. 3.2.1). ~~It turns out~~ In the previous section (Sect. 3.1.1), it is shown that the spatial distribution of the emission tracer for Southeast Asia has a fundamentally different behaviour than the distribution for emission tracers for North India, South India, and East China at 380 K potential temperature (see Fig. 5).

Figure 7 shows the horizontal distribution of emission tracers for North India (NIN) (left) and Southeast Asia (SEA) (right) at 380 K potential temperature over Asia for the four chosen days. In the early-phase on ~~1 July 2012 (top), 2 August 2012 (2nd row), 8 August 2012 (3rd row), and 20 September (bottom)~~. On 1 July 2012 (Fig. 7, top), air masses from boundary layer sources in North India and Southeast Asia are confined within the Asian monsoon anticyclone and within the filaments at its western and eastern flank. Air masses influenced by boundary layer sources from Southeast Asia are in addition found in the tropics. Within the anticyclone the emission tracer for Southeast Asia has the largest contribution at 380 K, followed by the emission tracers for North India. The contributions of the emissions tracer for South India is in the same order of magnitude as for North India and the lowest fraction is found for the emission tracer for East China (not shown here).

Similar as for 1 July 2012, on 2 August 2012 in the mid-phase at 380 K (Fig. 7, 2nd row, left) the distribution of the emission tracer for North India is also confined within the Asian monsoon anticyclone. Filaments containing enhanced contributions of the emission tracer for North India exist also at the western and eastern flank of the anticyclone. Contrary to the 1 July at the beginning of August, the highest percentages of emission tracers within the anticyclone are from North India and East China (not shown here), thus the impact of boundary sources located more northwards is larger than the impact of boundary sources from Southeast Asia and South India (not shown here).

Further on 2 August 2012 at 380 K, the spatial distribution of the emission tracers for North India shows two regions with maximum values, one in the core of the anticyclone over Iran and Afghanistan and another within the anticyclone farther northeast over China which is a remnant of a double peak structure found on 28 July 2012 as discussed above in Sect. 3.1.1.

~~In contrast~~ On 2 August 2012, the horizontal distribution of the emission tracer for Southeast Asia is completely different compared to the 1 July, ~~on~~ 2012. On 2 August 2012 (Fig. 7, 2nd row, right), the contributions of the emission tracer for Southeast Asia has a local minimum in the core of the anticyclone surrounded by enhanced percentages of the emission tracer for Southeast Asia ~~are found~~ at the edge of the anticyclone in particular at the southeast edge of the anticyclone and in the western and eastern filaments of the anticyclone. ~~Further looking at a wider geographical scale, large contributions of the emission tracer for Southeast Asia are found south of the anticyclone in the tropics, over the Pacific Ocean and west of the anticyclone over the South Atlantic Ocean. Low percentages of the emission tracer for Southeast Asia are found in the core of the anticyclone~~ This is in contrast to the emission tracer for North India (and East China, not shown here) having large contributions in the core. ~~The~~ and low values at the edge. Therefore, the spatial distribution of the emission tracer for Southeast Asia within the anticyclone is like a negative image to the spatial distribution of the emission tracer for North India. ~~Further looking at a wider geographical scale, large contributions of the emission tracer for Southeast Asia are found south of the anticyclone in the tropics, over the Pacific Ocean and west of the anticyclone over the South Atlantic Ocean.~~

On 8 August 2012 (Fig. 7, 3rd row), the Asian monsoon anticyclone is split into two smaller anticyclones. Apart from the double peak structure, the spatial distribution of the emission tracer for North India and Southeast Asia is similar to the distribution on 2 August 2012. ~~Remarkable~~ 2012, i. e. high contributions from North India and low contributions from Southeast Asia are found within both cores of the anticyclones. Also here, remarkable are high percentages of the emission tracer for Southeast Asia appear at the edge of the two anticyclones ~~and low percentages inside the two anticyclones~~. Thus at the beginning of

August 2012, the percentage of emission tracers for North India and East China (not shown here) outweigh the percentage of the emission tracers from further south for Southeast Asia and South India (not shown) inside the anticyclone in contrast to the conditions in [early the early-phase on 1 July](#).

Air masses originating in Southeast Asia can experience strong uplift by deep convection (e.g. Park et al., 2007; Li et al., 2005) or typhoons (Vogel et al., 2014). If an air parcel is uplifted at the edge of the Asian monsoon to altitudes high enough, it can be entrained into the anticyclonic circulation and subsequent clockwise transport of the air parcel around the outer edge of the anticyclone occurs. The edge of the anticyclone acts here as a strong transport barrier evident in the strong gradients of the different emission tracers at the edge of the anticyclone ([more details see Sect. ??](#)). The transport barrier acts in both directions, namely for inward transport apparent in the tracer distribution from Southeast Asia and for outward transport apparent in the tracer distribution for North India (see Fig. 7, 2nd and 3rd row). Further, air masses originating in the boundary layer in Southeast Asia are uplifted in the tropics at locations where they do not reach the Asian monsoon anticyclone. A subsequently isentropic poleward transport of these air masses from the tropics to the region of the Asian monsoon anticyclone is evident in the CLaMS simulation ([see Sect. ??](#)).

On [2012 September 2012](#) (see Fig. 7, bottom) [during the late-phase](#), the anticyclone is [shifted-broadened](#) to the south compared to the [location-area](#) of the Asian monsoon anticyclone in July and August. In the core of the Asian monsoon anticyclone, the main contributions are emission tracers for Southeast Asia and North India followed by East China (not shown). A smaller percentage is found for the emission tracer for South India (not shown). [Further, on 20 September 2012 \(see Fig. 7, bottom\), a strong eastward eddy shedding event occurred as discussed in the previous Sect. 3.1.1. In general during an eastward eddy shedding event, air masses from the core of the anticyclone can be mixed with air masses from the edge of the Asian monsoon anticyclone. Air masses separated in the second smaller anticyclone is transported eastwards by the subtropical jet to North America and Europe as discussed in Vogel et al. \(2014\).](#)

Further, on [2012](#) September 2012 at the end of the monsoon season, the spatial distribution of the emission tracer for Southeast Asia at 380 K is very different compared to the distributions of the emission tracer for North India in particular within the Northern Hemisphere. During the ~~end-of-the-monsoon-season~~[late-phase of the anticyclone](#), contributions of the emission tracers for North India are still trapped within the anticyclone. As discussed before, air masses originating in the boundary layer in Southeast Asia are uplifted both within the Asian monsoon anticyclone and elsewhere in the tropics. Uplift in the tropics and subsequent isentropic poleward transport at around 380 K yield propagation of air masses originating in the boundary layer of Southeast Asia to mid-latitudes(~~more details are discussed below in Sect. ??~~). Therefore, [the extratropical lowermost stratosphere in the Northern Hemisphere is flooded by end of September with air masses from Southeast Asia. as a result](#), high percentages of the emission tracer for Southeast Asia ~~is~~[are](#) more widely distributed compared to [the distribution of the](#) emission tracers for North India, South India and East China. ~~A movie showing the temporal evolution (on a daily basis) of the contribution of emission tracers for Southeast Asia at 380 potential temperature on the Northern Hemisphere during the Asian monsoon 2012 (1 May 2012–late October 2012) is available as a Supplement of this paper.~~

3.2.1 Temporal evolution of different emission tracers

After presenting the spatial distribution of the emission tracers for four selected days, we discuss the temporal evolution of different emission tracers within the Asian monsoon anticyclone in 2012. In the previous sections, it is shown that the area enclosed by the 4.5 PVU isoline constitutes a good upper boundary for the area within the Asian monsoon anticyclone at 380 K showing enhanced contributions of emission tracers for India/China within the Asian monsoon anticyclone. Ploeger et al. (2015) inferred a mean value of 3.8 PVU to mark the transport barrier for the Asian monsoon anticyclone 2012 at 380 K using the PV gradient and horizontal circulation. However, the PV value marking the transport barrier changes from day to day with maximum PV values up to 4.4–4.6 PVU and could only be deduced for a period from 20 June to 20 August 2012 (Ploeger et al., 2015). In [this our](#)

study, a value of 4.5 PVU is used which is in agreement with the upper limit of the PV values derived by Ploeger et al. (2015) and is extrapolated to early June and September/October 2012.

Therefore, to calculate the percentage of different emission tracers within the Asian monsoon anticyclone at 380 K, we use the following assumption. Mean values of all emission tracers are calculated in Asia for the region between 15 and 50° N and 0 and 140° E (at 380 ± 0.5 K, shown as black ~~box-rectangle~~ in Fig. 7). In addition to this geographical limit (black ~~box-rectangle~~), PV values lower than 4.5 PVU are required ~~to calculate for an air parcel to contribute to~~ the mean values of the different emission tracers within the Asian monsoon anticyclone for each day as shown in Fig. 8.

The contribution of different emission tracers from Asia within the anticyclone differ in time and from tracer to tracer (Fig. 8). The temporal evolution shows that significant contributions of the emission tracer for Southeast Asia (black) are found within the Asian monsoon anticyclone at 380 K potential temperature end of May that is roughly 2 weeks before contributions of the emission tracers for North India (red), South India (blue), and East China (green) reach at that level of potential temperature. At the beginning of the Asian monsoon period in June/early July, contributions of air masses originating in South Asia dominate within the anticyclone with maximum percentages of emission tracers on average of 13 % for Southeast Asia (black) and 6.5 % for South India (blue) at 380 K. During July 2012, the contributions of emission tracers for the south decrease to 10 % (Southeast Asia) and 6 % (South India) and contributions of emission tracers for the north, for North India (red) and East China (green) increase up to 18 and 10 %, respectively, until early August. During August 2012, the percentage of the emission tracers for the south rise again until the breakup of the anticyclone which occurred end of September in contrast to decreasing contributions of emission tracers for North India. Our simulations show that a south-north shift in the contribution of different emission tracers for Asia within the Asian monsoon anticyclone occurred during the summer 2012 and also a slight northward shift of the anticyclone itself. This behaviour is possibly linked to the northward moving long-term **intraseasonal**

interseasonal variations (30 to 60 day oscillations) found in climatological analyses of monsoon activity like convection and rainfall (e.g. Goswami, 2012, and references therein).

During August and September 2012, contributions of the emission tracer for North India (red) decrease in principle, ~~but show local maxima end of August and end of September. In the same time period, contributions of the emission tracer for East China show a slight increase with maximum percentages end of September. Thus in our simulations, an oscillation with a period of roughly~~ however short-term intraseasonal variations (10–20 days is found in the contributions of the emission tracer for North India during August and September) as a local phenomenon are found. We suggest that these oscillations are most likely connected to the short-term westward propagating intraseasonal variations (10–20 days) of the Asian summer monsoon found on a smaller horizontal scale (e.g. Goswami, 2012, and references therein). In the same time period, contributions of the emission tracer for East China show a slight increase with maximum percentages end of September.

At the end of September 2012, the contributions of emission tracers for North India, South India, and East China start to decrease caused by the breakup of the Asian monsoon anticyclone and the missing upward transport within the anticyclone. In contrast to these tracers, the contribution of emission tracers for Southeast Asia increases continuously up to 23 % from its minimum percentage of 10 % in late August until end of October. In early October, the anticyclone had already dissolved, however the contributions of the emission tracer for Southeast Asia still rise. The reason for this increase is that air masses originating in the boundary layer in Southeast Asia experienced in addition to the upward transport in the Asian monsoon anticyclone itself, uplift in the tropics and rapid uplift over the Pacific Ocean. The contribution of the emission tracer for the ~~background (grey line in Fig. 8, see Sect. 2.1.1)~~ also shows a strong increase Tropic Pacific Ocean (TPO) increases after the breakup of the anticyclone indicating an (yellow) indicating a strong uplift of air masses outside of Asia in the tropical Pacific. The influence of other land masses (yellow + tropical Atlantic and Indian Ocean (dark grey) line in Fig. 8) and of the background (light grey) is of minor importance throughout the considered time period. ~~Note that the sum of~~

~~all emission tracers shown in Fig. 8 is less than 100 because air masses originating in the free troposphere or stratosphere also contribute.~~

The conclusions deduced from the temporal evolution of emission tracers does do not depend on the precise value of 4.5 PVU. Very similar results were obtained for a choice of 3.8 PVU. Further, even if no PV criterion is applied and all air parcels within the geographical limits (black box rectangle in Fig. 2, 3, and 7) are considered to calculate the mean values, the same qualitative evolution emerges of the contributions of different emission tracers emerges within the anticyclone at 380 K, ~~however the contributions of the different emission tracers are in general lower (not shown here).~~

~~In this section, we could answer our first question of what is the impact of different boundary layer sources in Asia to the Asian monsoon anticyclone in summer 2012. Our simulations show first that emissions from North India (NIN), South India (SIN), East China (EGH), and Southeast Asia (SEA) have an significant impact on the Asian monsoon anticyclone. The contributions of the different emission tracers are highly variable in time, but in general the highest contributions are from North India and Southeast Asia at 380. In the early (June to mid-July) and late period (mid-August to October) of the monsoon season 2012, However then using only the geographical limits, highest contributions from Southeast Asia up to 11% and 19% are calculated in mid-June/mid-July and October, respectively. The contribution of air masses originating in Southeast Asia are highest and from North India has also its maximum in the intervening period (≈August 2012) contributions from North India have the largest impact indicating a south-north shift of the convection. Short-term intraseasonal variations (10–20) as a local phenomenon are found in the emission tracer for North India.~~

3.2.2 CLaMS results at 360 and 400K

from mid-July to mid-August and reaches values up to 13% (not shown here).

~~In Sect. 3.2, we discussed the contributions of different The artificial emission tracers in CLaMS are designed to identify possible boundary source regions in Asia that could contribute to the composition of the Asian monsoon anticyclone at a level of 380potential~~

temperature. Here, we briefly discuss the CLaMS results for lower (360) and higher (400) levels of potential temperature as shown in Figs. ?? and ??.

In general, the location and shape of the anticyclone at 360 and 400 are nearly identical. The spatial distributions of emission tracers for India/China (here the sum of North India (NIN), South India (SIN), and East China (ECH)) are confined within the anticyclone similar to 380 potential temperature, however the percentages are higher at 360 and lower at 400 (see Fig. ??). Highest percentages during the monsoon season 2012 (as defined in Sect. 2.1.1) considering advection and mixing processes. For example, the contribution of the emission tracer for India/China are found in the core of the anticyclone, indicating a slow upward transport of emissions from India/China within the Asian monsoon anticyclone.

The distribution of the emission tracer for Southeast Asia (see Fig. ??) within the anticyclone is different compared to the distribution of the emission tracers for India/China (see Fig. ??). In addition to the convectively driven uplift within the Asian monsoon, air masses from Southeast Asia experience further upward transport pathways. First, strong convective uplift occurred in the Pacific (Li et al., 2005) e.g. caused by typhoons (Vogel et al., 2014) at the southeast flank of the Asian monsoon anticyclone. Afterwards these emissions can be entrained into the outer circulation of Southeast Asia dominates in June, demonstrating that in June upward transport or convection is comparably strong in Southeast Asia compared to other regions in Asia. By this technique contributions of the boundary layer with a transport time from the boundary to the UTLS longer than one monsoon period (contributions from the boundary layer that are released before 1 May 2012) are not covered by the artificial tracers used here. Therefore, the composition of different emission tracers within the Asian monsoon anticyclone and are transported clockwise at the edge of the circulation around the core of is a fingerprint of the regional and temporal variations of convective processes causing strong upward transport within the Asian monsoon anticyclone. Therefore in general, a high percentage of the emission tracer for Southeast Asia is found at the edge of the Asian monsoon anticyclone as evident at 360 (see in summer 2012).

The sum of all emission tracers shown in Fig. ??, left). This finding is consistent with backward trajectory calculations by Vogel et al. (2014) for the same time period, that show that 8 is less than 100 % because air masses originating in Southeast Asia circulate in an upward spiral around the core of the free troposphere or stratosphere also contribute to the composition of Asian monsoon anticyclone. In contrast, at 400 For the end of June, a contribution of 35 potential temperature, high percentages of air masses originating in Southeast Asia are found within the anticyclone similar as for the emission tracer for India/China and lower contributions of the emission tracer for Southeast Asia are found outside the anticyclone. This indicates an upward transport of air masses from Southeast Asia at the edge of the anticyclone up to the top of the anticyclone at around 400% of the model boundary layer to the composition of the Asian monsoon anticyclone is calculated. The remaining 65 in contrast to the upward transport of air masses from India/China within the core % of the composition of the anticyclone is from the free troposphere and the stratosphere.

A second upward transport pathways for the emission tracer for Southeast Asia is uplift of in the deep tropics. Its impact on the chemical composition of lowermost stratosphere is discussed in the next Sect. ??.

3.3 Transport pathways to the lowermost stratosphere

3.2.1 Flooding of the Northern Hemisphere

The spatio-temporal evolution of air masses originating in the boundary layer in Southeast Asia is very different from air masses originating in India/China since Southeast Asia is located at the southeast edge of the Asian monsoon anticyclone, towards the tropics (12 The contribution of the model boundary layer rises up to 55 S–20% in early August and up to 75 N) as shown in Figs. ?? and ??.

At % at the end of the monsoon season in late September. Thus at the end of the Asian monsoon season on 20 September monsoon season 2012, air masses with high percentages of the emission tracers for India/China (see Fig. ??, bottom) are trapped

within the chemical composition of the Asian monsoon anticyclone ~~except for the release of filaments or eddy-shedding events that transport air masses out of the anticyclone to either the west or to the east (outflow of the Asian monsoon).~~ In contrast, Fig. ?? (bottom) shows that at the end of the Asian monsoon period air masses with enhanced contributions from boundary layer sources in Southeast Asia are found globally in the upper troposphere from the tropics to the tropical side of the subtropical jet in both hemispheres at 360, 380 and 400. is dominated by contributions of the model boundary layer uplifted during the course of the monsoon season 2012.

Air masses originating in Southeast Asia are uplifted in the deep tropics. Afterwards they spread out within the tropics and subsequent isentropic transport to high latitudes occurs most likely associated with the lower branch of the Brewer–Dobson circulation (Fig. ??). At 360 and 380, the contribution of the emission tracer for Southeast Asia shows no strong gradient at the southern flank of the anticyclone (Fig. ??, bottom left/middle) in contrast to the emission tracer for India/China (Fig. ?? bottom left/middle). Thus the gradient of the emission tracer for Southeast Asia at the southern edge

4 Conclusions

In this paper, the impact of different boundary layer source regions in Asia to the composition of the Asian monsoon anticyclone ~~is weaker at 360 and 380 compared to the gradient for emission tracers for India/China. Air masses originating in the boundary layer in Southeast Asia can be uplifted both within the anticyclone and outside, so that the southern edge of the anticyclone is masked.~~

In contrast, at 400a strong gradient is found at the southern flank of the anticyclone in the distribution of the emission tracer for Southeast Asia suggesting that at this level the isentropic transport from the tropics to higher latitudes is weaker than below at the level of 380 potential temperature. As a result, the Northern and Southern Hemisphere are flooded around 380 with air masses originating in the boundary layer of Southeast Asia; that means that air masses are younger in September than before the Asian monsoon

season at that level of potential temperature. Thus in the Northern Hemisphere, air masses from Southeast Asia are uplifted in the tropics and widely distributed around the anticyclone caused by the anticyclonic flow in this region acting as a large stirrer. The subtropical jets in both hemispheres act as [2012 is characterised by CLaMS model simulations using artificial emissions tracers. Our simulations show that the Asian monsoon anticyclone is highly variable in location and shape and the edge of the anticyclone constitutes a remarkable strong transport barrier for transport from the upper troposphere into the lowermost stratosphere. This quasi-horizontal transport of air masses from the tropical tropopause layer \(TTL\) to higher latitudes yields moistening of the extratropical lowermost stratosphere \(e.g. Ploeger et al., 2013; ?\) artificial emission tracers.](#)

Moreover, air masses from the the Asian monsoon anticyclone including air masses originating in Southeast Asia and also from India/China can be separated from the main circulation at its northern flank by eastward eddy shedding or release of filaments. These wet and polluted air masses are transported eastwards along the subtropical jets (e.g. Vogel et al., 2014) and can be transported most likely by Rossby wave breaking into the lowermost stratosphere. Afterwards, enhanced contributions of [The calculated correlation coefficients indicate good agreement between the horizontal distributions of simulated CO₂, O₃ and artificial emission tracers for Asia are found in the extratropical lowermost stratosphere.](#)

After the breakup of the Asian monsoon anticyclone in October 2012, also air masses with contributions from boundary emission from North India, South India, and East China that were trapped before within the anticyclone are distributed globally within the lowermost stratosphere (see Fig. 3, bottom left, and animations in the Supplement of this paper).

4.0.1 Gateways for air masses from the anticyclone to the stratosphere

Possible vertical transport at the top of the Asian monsoon anticyclone around the tropopause and possible isentropic transport at the edge of the anticyclonic circulation is discussed analysing the spatial distribution of emission tracers for Asia in CLaMS. We have chosen the 20 September 2012 as an example, already shown in Figs. 3 (top)

and 7 (bottom). Figure ?? shows latitude-height cross-sections across the area of the Asian Monsoon anticyclone at 80E longitude of (a) static stability (buoyancy frequency squared, N^2), the contributions of the emission tracers for (b) India/China (=North India (NIN)+South India (SIN)+East China (ECH); see Sect. 2.1.1), (c) Southeast Asia (SEA); and (d) Siberia (SIB) on 20 September 2012. Figure ??a shows that the thermal tropopause (black dots) above the anticyclone ($\approx 15-35N$) is elevated (e.g. ??). The anticyclone is flanked by the subtropical westerly jet in the north ($\approx 30-40N$) and the equatorial easterly jet in the south ($\approx 0-10N$) (wind velocities of both jets are shown as black lines). Further at its northern flank, a double thermal tropopause (at ≈ 340 China with patterns found in satellite measurements of O_3 and CO by the Aura Microwave Limb Sounder (MLS). For the monsoon season, correlation coefficients $r(t)$ of 0.72-0.86 and 400 potential temperature) is found between 40-0.57-0.81 were calculated for $MLS(O_3)/CLaMS(O_3)$ and 60N. Multiple tropopauses occur often at the northern flank of the Asian monsoon anticyclone along the subtropical jet (e.g. ?). The potential temperature level at 380 is marked as a purple line to illustrate the position of the horizontal cross-sections shown in Figs. 3 (top) and 7 (bottom). The 380 level is just below the thermal tropopause (black dots) in the tropics and within the Asian monsoon anticyclone, however north of the anticyclone it is above the first tropopause and therefore within the lowermost stratosphere. In general, tropospheric air masses, including air masses within the both $MLS(CO)/CLaMS(CO)$ and $MLS(CO)/CLaMS(India/China)$ correlations, respectively. The good correlation found between the emission tracer for India/China and MLS measurements as well as PV confirms that the spatial distribution of the emission tracer for India/China is a good proxy for the location and shape of Asian monsoon anticyclone, are characterised by low values of N^2 in contrast to stratospheric air masses. High values (dark red) of N^2 found directly above the first tropopause characterise the tropopause inversion layer (TIL) (e.g. ?). Figure ??a shows that sandwiched between the double tropopause at the northern flank of the anticyclone low values of N^2 (shown in blue/green) occur in comparison to the stratospheric background on 20 September 2012 indicating that tropospheric air masses

from the Asian monsoon anticyclone was isentropically transported into the lowermost stratosphere.

Figure ??b shows that high percentages of the emission tracers for India/China are transported upward within the Asian monsoon anticyclone up to the thermal tropopause and are trapped within the anticyclone (≈ 15 – 35 N). Enhanced contributions of the emissions tracers for India/China are in addition found on the Southern Hemisphere on the equatorial flank of the subtropical jet, indicating additional upward transport elsewhere in the tropics.

In contrast, air masses originating in the boundary layer in Southeast Asia (see Fig. ??c) are released at latitudes lower (12 S– 20 N) than air masses originating in India/China (0– 40 N) therefore air masses from Southeast Asia are uplifted both within the Asian monsoon anticyclone and elsewhere in the tropics. High percentages of the emission tracer for Southeast Asia are found up to ≈ 50 at early-July to early-August (mid-phase) is found. Further in early-September, during the late-phase of the anticyclone, a much broader spatial distribution is found, in particular the southern edge of the anticyclone, up to ≈ 20 within the anticyclone, and up to ≈ 25 – 30 elsewhere in is shifted to the tropics. Figure ??c shows that the upward transport of air masses originating in Southeast Asia within the Asian monsoon anticyclone can not be isolated from the transport in the deep tropics as also reported by Gettelman et al. (2004) and Bannister et al. (2004).

Further, Fig. ??b and c shows that the thermal tropopause acts as a transport barrier for emission tracers for India/China and Southeast Asia. Only a very shallow mixing layer is found around the tropopause above the anticyclone (≈ 15 – 35 N). Therefore the tropopause constitutes an upper boundary of the Asian monsoon anticyclone as expected from satellite measurements of tropospheric trace gases (see Sect. 1). In the deep tropics (≈ 10 – 25 S), enhanced percentages of After the breakup of the anticyclone in early-October, still high percentages for the emission tracer for India/China and Southeast Asia are found above the tropopause (≈ 380) in late-September, indicating a possible vertical upward transport into the stratosphere over the course of 5 months of CLaMS simulation.

Figure ??b and c shows enhanced contributions of emission tracers for both India/China and Southeast Asia north of the Asian monsoon anticyclone between the double tropopause and further to the north at higher latitudes indicating an isentropic transport of trace gases from the anticyclone into the lowermost stratosphere as already indicated by N_2 (see Fig. ??a). In contrast, contributions of the emission tracer for Siberia (see Fig. ??d) are not found in the lowermost stratosphere confirming that in mid- and high latitudes the first troposphere acts as a transport barrier and that vertical upward transport from boundary source emissions from the troposphere into the lowermost stratosphere seems unlikely. Enhanced contributions of emission tracers from India/China and Southeast Asia are found between double tropopauses and on the polar side of the anticyclone at corresponding levels of potential temperature, however the exact locations and mechanisms for stratospheric entry are not clear. One possibility could be horizontal transport of air masses from the Asian monsoon anticyclone between double tropopauses into the lowermost stratosphere (e.g. ?). In previous studies (e.g. ?Vogel et al., 2011b), it was shown that air masses with enhanced tropospheric characteristics from the tropical upper troposphere or tropical transition layer (TTL) are found between double tropopauses indicating an horizontal transport of tropospheric air masses into the lowermost stratosphere.

A second mechanism could be the clockwise transport of boundary emissions in form of an upward spiral around the core of the Asian monsoon anticyclone of air masses lifted at the outer edge of the anticyclonic e.g. by typhoons or deep convection (Li et al., 2005; Vogel et al., 2014) as evident in our simulation for emissions from Southeast Asia. Or third, the transport mechanism is a mixture of point one and two. To answer this question, further investigations and measurements focusing on transport processes at the edge of the Asian monsoon anticyclone, in particular at its northern flank, are necessary.

In this paper, are located over India, China and the Pacific Ocean.

In this paper, we could answer the question of what is the impact of different boundary layer source regions sources in Asia to the composition of the Asian monsoon anticyclone 2012 is characterised by CLAMS model simulations using artificial emissions

tracers. Our simulations show that the Asian monsoon anticyclone is highly variable in location and shape and oscillates between two states with a time period of $\approx 10\text{--}30$: first a symmetric anticyclone and second, an asymmetric anticyclone either elongated or split in two smaller anticyclones. A maximum in the distribution of air originating from Indian/Chinese boundary layer sources is usually found in the core of a symmetric anticyclone, in contrast an asymmetric state is characterised by a double peak structure in the horizontal distribution of air originating from India and China. In our simulations, the edge of the anticyclone constitutes for both states a remarkable strong transport barrier. Measurements of and by the Aura Microwave Limb Sounder (MLS) show the same patterns as emission tracers for India/China over Asia. We suggest that this behaviour is caused by the intraseasonal variability of the Asian summer monsoon related to its active and break phases (, e.g.) and references therein Goswami2012. Evidence of a bimodal distribution depending on longitude is found in the contribution of emission tracers for India/China at 380 similar as found for the location of the anticyclone core derived by ?.

Further, the in summer 2012. The model results show that emissions from North India, South India, East China, and Southeast Asia have an impact on the composition of the Asian monsoon anticyclone in contrast to all other land masses. The contributions of these different emission tracers on the composition of the anticyclone are highly variable in time, but in general the highest contribution are from North India and Southeast Asia. In the early (\approx June to mid-July) and late period (\approx mid-August to September/October) of the monsoon season 2012, contributions from Southeast Asia are highest (up to 13% and 23%, respectively, using a value of 4.5 PVU to mark the edge of the anticyclone). In the intervening period (\approx mid-July to mid-August), air masses from North India have the strongest impact contribution to the composition of the anticyclone (up to 18%). This behaviour is likely caused by the large scale northward moving 30 to 60 day oscillations of the Asian monsoon evident in repeatedly northward-propagating wet spells during the summer monsoon season. Short-term intraseasonal variations (10–20 days) are found in the contribution for air masses originating in North India, which is likely associated to westward propagating 10 to 20 day oscillations of the South Asian summer monsoon found on a smaller horizontal scale.

Our simulation confirms that both North India including the Tibetan Plateau (Bergman et al., 2013) and Southeast Asia including the eastern part of Bay of Bengal, South Asian subcontinent, Western Pacific, and the Philippine Seas (Park et al., 2009; Chen et al., 2012) are important source regions for the chemical composition of the Asian monsoon anticyclone. Our simulations demonstrate that the contributions of different boundary ~~sources~~ source regions to the composition of the Asian monsoon anticyclone show strong intraseasonal variations. Thus the chemical contribution of the Asian monsoon anticyclone is a fingerprint of the regional temporal variation of convective processes. Therefore the processes are more complex than hitherto believed.

In addition, emissions from Southeast Asia are found both within the Asian monsoon anticyclone and at the outer edge of the anticyclone. CLaMS simulations show that emissions from Southeast Asia can be rapidly uplifted by deep convection (Li et al., 2005; Chen et al., 2012) or typhoons (Vogel et al., 2014) up to the outer edge of the anticyclone (at around 380 K). Afterwards, the emissions are entrained by the anticyclonic circulation of the Asian monsoon and circulate clockwise, in an upward spiral, at the edge of the Asian monsoon anticyclone around its core (this is also true if the anticyclone is split into two smaller anticyclones).

~~Further, our simulations confirm that the thermal tropopause above the anticyclone constitutes a vertical transport barrier, as expected from satellite observations (e.g. Rosenlof et al., 1997; Jackson et al., 1998; Park et al., 2004, 2008; Li et al., 2005; Xiong et al., 2005). Upward transport of air masses from India/China or Southeast Asia into the lower stratosphere can occur in the deep tropics by entrainment into the upward Brewer–Dobson circulation, however the time scales to reach altitudes much higher than 400 potential temperature are longer than one monsoon season. Furthermore, in our simulations enhanced contributions of emission tracers for India/China and Southeast Asia are found at the northern flank of the Asian monsoon anticyclone between double tropopauses indicating an isentropic transport from the anticyclone into the lowermost stratosphere.~~

Moreover, our ~~simulation shows~~ simulations show that air masses originating in Southeast Asia can be uplifted elsewhere in the deep tropics and subsequently spread out during

the simulation globally on the tropical side of the subtropical jet ~~streams in both hemispheres~~ stream at around 380 K, in contrast to emissions from North India, South India, and East China that are trapped in the Asian monsoon anticyclone. During the summer 2012, this mechanism caused flooding of the lowermost stratosphere with relatively young air masses ~~carrying moisture and pollution from~~ originating in Southeast Asia. Finally, after the breakup of the Asian monsoon anticyclone ~~in October~~ proceed in late September 2012, also emissions from North India, South India, and East China that were trapped before within the Asian monsoon anticyclone were distributed globally within the UTLS.

Our findings demonstrate that emissions from India/China and Southeast Asia carrying moisture and pollution affected by the circulation of the Asian monsoon anticyclone have a significant impact on the chemical compositions of the lowermost stratosphere of the Northern Hemisphere in particular at end of the monsoon season in September/October 2012. ~~The resulting moistening of the the lowermost stratosphere has a potential impact on surface climate (e.g. Solomon et al., 2010; Riese et al., 2012).~~

The Supplement related to this article is available online at [doi:10.5194/acpd-0-1-2015-supplement](https://doi.org/10.5194/acpd-0-1-2015-supplement).

Acknowledgements. The authors sincerely thank Paul Konopka, Felix Plöger, and Reinhold Spang (all at Research Centre Jülich) for helpful discussions. We thank the MLS scientific team (Aura Microwave Limb Sounder) for providing satellite data and the European Centre of Medium-Range Weather Forecasts (ECMWF) for providing the ERA-Interim reanalysis data. The authors gratefully acknowledge the computing time granted on the supercomputer JUROPA at Jülich Supercomputing Centre (JSC) under the VSR project ID JICG11. Our activities were partly ~~founded~~ funded by the German Science Foundation (Deutsche Forschungsgemeinschaft, DFG) under the DFG project LASSO (HALO-SPP 1294/GR 3786). ~~This work also supports the campaign activities within the StratoGlim project funded by the European Commission (under grant number StratoGlim-603557-FP7-ENV.2013.6.1-2).~~

The article processing charges for this open-access publication were covered by a Research Centre of the Helmholtz Association.

References

- Annamalai, H. and Slingo, J. M.: Active/break cycles: diagnosis of the intraseasonal variability of the Asian Summer Monsoon, *Clim. Dynam.*, 18, 85–102, 2001.
- Bannister, R. N., O'Neill, A., Gregory, A. R., and Nissen, K. M.: The role of the south-east Asian monsoon and other seasonal features in creating the “tape-recorder” signal in the Unified Model, *Q. J. Roy. Meteor. Soc.*, 130, 1531–1554, 2004.
- Bergman, J. W., Fierli, F., Jensen, E. J., Honomichl, S., and Pan, L. L.: Boundary layer sources for the Asian anticyclone: regional contributions to a vertical conduit, *J. Geophys. Res.*, 118, 2560–2575, doi:10.1002/jgrd.50142, 2013.
- Bian, J., Pan, L. L., Paulik, L., Vömel, H., and Chen, H.: In situ water vapor and ozone measurements in Lhasa and Kunmin during the Asian summer monsoon, *Geophys. Res. Lett.*, 39, L19808, doi:10.1029/2012GL052996, 2012.
- ~~Birner, T., Sankey, D., and Shepherd, T. G.: The tropopause inversion layer in models and analyses, *Geophys. Res. Lett.*, 33, L14804, 2006.~~
- Bourassa, A. E., Robock, A., Randel, W. J., Deshler, T., Rieger, L. A., Lloyd, N. D., Llewellyn, E. J. T., and Degenstein, D. A.: Large volcanic aerosol load in the stratosphere linked to Asian monsoon transport, *Science*, 337, 78–81, doi:10.1126/science.1219371, 2012.
- Brasseur, G. and Solomon, S.: *Aeronomy of the Middle Atmosphere: Chemistry and Physics of the Stratosphere and Mesosphere*, 3rd edn., Springer, Heidelberg, Germany, 2005.
- Chen, B., Xu, X. D., Yang, S., and Zhao, T. L.: Climatological perspectives of air transport from atmospheric boundary layer to tropopause layer over Asian monsoon regions during boreal summer inferred from Lagrangian approach, *Atmos. Chem. Phys.*, 12, 5827–5839, doi:10.5194/acp-12-5827-2012, 2012.
- Dee, D. P., Uppala, S. M., Simmons, A. J., Berrisford, P., Poli, P., Kobayashi, S., Andrae, U., Balmaseda, M. A., Balsamo, G., Bauer, P., Bechtold, P., Beljaars, A. C. M., van de Berg, L., Bidlot, J., Bormann, N., Delsol, C., Dragani, R., Fuentes, M., Geer, A. J., Haimberger, L., Healy, S. B., Hersbach, H., Holm, E. V., Isaksen, I., Kallberg, P., Koehler, M., Matricardi, M., McNally, A. P., Monge-Sanz, B. M., Morcrette, J.-J., Park, B.-K., Peubey, C., de Rosnay, P., Tavolato, C., Thep-

- aut, J.-N., and Vitart, F.: The ERA-Interim reanalysis: configuration and performance of the data assimilation system, *Q. J. Roy. Meteor. Soc.*, 137, 553–597, doi:10.1002/qj.828, 2011.
- Dethof, A., O’Neill, A., Slingo, J. M., and Smit, H. G. J.: A mechanism for moistening the lower stratosphere involving the Asian summer monsoon, *Q. J. Roy. Meteor. Soc.*, 556, 1079–1106, 1999.
- ~~Dunkerton, T. J.: Evidence of meridional motion in the summer lower stratosphere adjacent to monsoon regions, *J. Geophys. Res.*, 100, 16675–16688, 1995.~~
- Dvortsov, V. L. and Solomon, S.: Response of the stratospheric temperatures and ozone to past and future increases in stratospheric humidity, *J. Geophys. Res.*, 106, 7505–7514, 2001.
- Fadnavis, S., Semeniuk, K., Pozzoli, L., Schultz, M. G., Ghude, S. D., Das, S., and Kakatkar, R.: Transport of aerosols into the UTLS and their impact on the Asian monsoon region as seen in a global model simulation, *Atmos. Chem. Phys.*, 13, 8771–8786, doi:10.5194/acp-13-8771-2013, 2013.
- Fadnavis, S., Schultz, M. G., Semeniuk, K., Mahajan, A. S., Pozzoli, L., Sonbawne, S., Ghude, S. D., Kiefer, M., and Eckert, E.: Trends in peroxyacetyl nitrate (PAN) in the upper troposphere and lower stratosphere over southern Asia during the summer monsoon season: regional impacts, *Atmos. Chem. Phys.*, 14, 12725–12743, doi:10.5194/acp-14-12725-2014, 2014.
- Fairlie, T. D., Vernier, J.-P., Natarajan, M., and Bedka, K. M.: Dispersion of the Nabro volcanic plume and its relation to the Asian summer monsoon, *Atmos. Chem. Phys.*, 14, 7045–7057, doi:10.5194/acp-14-7045-2014, 2014.
- Forster, P. and Shine, K. P.: Stratospheric water vapour change as possible contributor to observed stratospheric cooling, *Geophys. Res. Lett.*, 26, 3309–3312, doi:10.1029/1999GL010487, 1999.
- Forster, P. and Shine, K. P.: Assessing the climate impact of trends in stratospheric water vapor, *Geophys. Res. Lett.*, 29, 10-1–10-4, doi:10.1029/2001GL013909, 2002.
- Fromm, M., Kablick III, G., Nedoluha, G., Carboni, E., Grainger, R., Campbell, J., and Lewis, J.: Correcting the record of volcanic stratospheric aerosol impact: Nabro and Sarychev Peak, *J. Geophys. Res.*, 119, 10343–10364, doi:10.1002/2014JD021507, 2014.
- Garny, H. and Randel, W. J.: Dynamic variability of the Asian monsoon anticyclone observed in potential vorticity and correlations with tracer distributions, *J. Geophys. Res.*, 118, 13421–13433, doi:10.1002/2013JD020908, 2013.
- Gottelman, A., Kinnison, D., Dunkerton, T. J., and Brasseur, G. P.: Impact of monsoon circulations on the upper troposphere and lower stratosphere, *J. Geophys. Res.*, 109, D22101, doi:10.1029/2004JD004878, 2004.

- Goswami, B. N.: South Asian monsoon, in: *Intraseasonal Variability in the Atmosphere-Ocean Climate System*, 2nd edn., chap. 2, edited by: Lau, W. K. M. and Waliser, D. E., Springer-Verlag, Berlin, Heidelberg, 21–72, 2012.
- Grooß, J.-U. and Müller, R.: Simulation of ozone loss in Arctic winter 2004/2005, *Geophys. Res. Lett.*, 34, L05804, doi:10.1029/2006GL028901, 2007.
- Grooß, J.-U., Konopka, P., and Müller, R.: Ozone chemistry during the 2002 Antarctic vortex split, *J. Atmos. Sci.*, 62, 860–870, 2005.
- Grooß, J.-U., Engel, I., Borrmann, S., Frey, W., Günther, G., Hoyle, C. R., Kivi, R., Luo, B. P., Molleker, S., Peter, T., Pitts, M. C., Schlager, H., Stiller, G., Vömel, H., Walker, K. A., and Müller, R.: Nitric acid trihydrate nucleation and denitrification in the Arctic stratosphere, *Atmos. Chem. Phys.*, 14, 1055–1073, doi:10.5194/acp-14-1055-2014, 2014.
- Günther, G., Müller, R., von Hobe, M., Strohm, F., Konopka, P., and Volk, C. M.: Quantification of transport across the boundary of the lower stratospheric vortex during Arctic winter 2002/2003, *Atmos. Chem. Phys.*, 8, 3655–3670, doi:10.5194/acp-8-3655-2008, 2008.
- Hegglin, M. I., and Tegtmeier, S. (Eds.): SPARC Data Initiative: Assessment of Stratospheric Trace Gas and Aerosol Climatologies from Satellite Limb Sounders, SPARC Report No. 7, in preparation, 2015.
- ~~Highwood, E. J. and Hoskins, B. J.: The tropical tropopause, *Q. J. Roy. Meteor. Soc.*, 124, 1579–1604, 1998.~~
- ~~Holton, J. R., Haynes, P., McIntyre, M. E., Douglass, A. R., Rood, R. B., and Pfister, L.: Stratosphere-troposphere exchange, *Rev. Geophys.*, 33, 403–439, 1995.~~
- ~~Hsu, C. J. and Plumb, R. A.: Nonaxisymmetric thermally driven circulations and upper-tropospheric monsoon dynamics, *J. Atmos. Sci.*, 57, 1255–1276, 2001.~~
- Jackson, D. R., Driscoll, S. J., Highwood, E. J., Harries, J. E., and Russell III, J. M.: Troposphere to stratosphere transport at low latitudes as studies using HALOE observations of water vapor 1992–1997, *Q. J. Roy. Meteor. Soc.*, 124, 169–192, 1998.
- Kirk-Davidoff, D. B., Hints, E. J., Anderson, J. G., and Keith, D. W.: The effect of climate change on ozone depletion through changes in stratospheric water vapour, *Nature*, 402, 399–401, doi:10.1038/46521, 1999.
- Konopka, P. and Pan, L. L.: On the mixing-driven formation of the Extratropical Transition Layer (ExTL), *J. Geophys. Res.*, 117, D18301, doi:doi:10.1029/2012JD017876, 2012.
- Konopka, P., Grooß, J.-U., Günther, G., Plöger, F., Pommrich, R., Müller, R., and Livesey, N.: Annual cycle of ozone at and above the tropical tropopause: observations

- versus simulations with the ~~Chemical Lagrangian Model of the Stratosphere (CLAMS)~~[Chemical Lagrangian Model of the Stratosphere \(CLAMS\)](#), *Atmos. Chem. Phys.*, 10, 121–132, [doi](#):, 2010.
- Konopka, P., Ploeger, F., and Müller, R.: Entropy- and static stability-based Lagrangian model grids, in: *Geophysical Monograph Series: Lagrangian Modeling of the Atmosphere*, vol. 200, edited by ~~Lin~~, edited by Lin, J., vol. 200, pp. 99–109, American Geophysical Union, 99–109, [doi](#):, doi:10.1029/2012GM001253, 2012.
- [Kumar, K. K., Rajagopalan, B., Hoerling, M., Bates, G., and Cane, M.: Unraveling the Mystery of Indian Monsoon Failure During El Niño, *Science*, 314, 115–119, doi:10.1126/science.1131152, 2006.](#)
- Li, Q., Jiang, J. H., Wu, D. L., Read, W. G., Livesey, N. J., Waters, J. W., Zhang, Y., Wang, B., Filipiak, M. J., Davis, C. P., Turquety, S., Wu, S., Park, R. J., Yantosca, R. M., and Jacob, D. J.: Convective outflow of South Asian pollution: a global CTM simulation compared with EOS MLS observations, *Geophys. Res. Lett.*, 32, L14826, doi:10.1029/2005GL022762, 2005.
- Liu, Y., Wang, Y., Liu, X., Cai, Z., and Chance, K.: Tibetan middle tropospheric ozone minimum in June discovered from GOME observations, *Geophys. Res. Lett.*, 36, L05814, doi:10.1029/2008GL037056, 2009.
- Livesey, N. J., Filipiak, M. J., Froidevaux, L., Read, W. G., Lambert, A., Santee, M. L., Jiang, J. H., Pumphrey, H. C., Waters, J. W., Cofield, R. E., Cuddy, D. T., Daffer, W. H., Drouin, B. J., Fuller, R. A., Jarnot, R. F., Jiang, Y. B., Knosp, B. W., Li, Q. B., Perun, V. S., Schwartz, M. J., Snyder, W. V., Stek, P. C., Thurstans, R. P., Wagner, P. A., Avery, M., Browell, E. V., Cammas, J.-P., Christensen, L. E., Diskin, G. S., Gao, R.-S., Jost, H.-J., Loewenstein, M., Lopez, J. D., Nedelec, P., Osterman, G. B., Sachse, G. W., and Webster, C. R.: Validation of Aura Microwave Limb Sounder O_3 and CO observations in the upper troposphere and lower stratosphere, *J. Geophys. Res.*, 113, D15S02, [doi](#):doi:10.1029/2007JD008805, 2008.
- ~~Livesey,~~
- [Livesey,](#) N. J., Read, W. G., Froidevaux, L., Lambert, A., Manney, G. L., Pumphrey, H. C., Santee, M. L., Schwartz, M. J., Wang, S., Cofield, R. E., Cuddy, D. T., Fuller, R. A., Jarnot, R. F., Jiang, J. H., Knosp, B. W., Stek, P. C., Wagner, P. A., and Wu, D. L.: EOS MLS Version 3.3 Level 2 data quality and description document, Tech. rep., Jet Propulsion Laboratory, available [at: from](#) https://mls.jpl.nasa.gov/data/v3-3_data_quality_document.pdf, 2011.
- ~~Manney, G. L., Hegglin, M. I., Daffer, W. H., Schwartz, M. J., Santee, M. L., and Pawson, S.: Climatology of Upper Tropospheric-Lower Stratospheric (UTLS) jets and tropopause in MERRA, *J. Climate*, 27, 3248–3271, doi:, 2014.~~

- McKenna, D. S., Grooß, J.-U., Günther, G., Konopka, P., Müller, R., Carver, G., and Sasano, Y.: A new Chemical Lagrangian Model of the Stratosphere (CLaMS): 2. Formulation of chemistry scheme and initialization, *J. Geophys. Res.*, 107, 4256, doi:10.1029/2000JD000113, 2002a.
- McKenna, D. S., Konopka, P., Grooß, J.-U., Günther, G., Müller, R., Spang, R., Offermann, D., and Orsolini, Y.: A new Chemical Lagrangian Model of the Stratosphere (CLaMS): 1. Formulation of advection and mixing, *J. Geophys. Res.*, 107, 4309, doi:10.1029/2000JD000114, 2002b.
- ~~Nash, E. R., Newman, P. A., Rosenfield, J. E., and Schoeberl, M. R.: An objective determination of the polar vortex using Ertel's potential vorticity, *J. Geophys. Res.*, 101, 9471–9478, 1996.~~
- Pan, L. L., Konopka, P., and Browell, E. V.: Observations and model simulations of mixing near the extratropical tropopause, *J. Geophys. Res.*, 111, D05106, doi:10.1029/2005JD006480, 2006.
- ~~Pan, L. L., Randel, W. J., Gille, J. C., Hall, W. D., Nardi, B., Massie, S., Yudin, V., Khosravi, R., Konopka, P., and Tarasick, D.: Tropospheric intrusions associated with the secondary tropopause, *J. Geophys. Res.*, 112, D10302, doi:, 2009.~~
- Park, -M., Randel, -W. J., Kinnison, -D. E., Garcia, -R. R., and Choi, -W.: Seasonal variation of methane, water vapor, and nitrogen oxides near the tropopause: Satellite observations and model simulations, *J. Geophys. Res.*, 109, D03302, doi:doi:10.1029/2003JD003706, 2004.
- Park, -M., Randel, -W. J., Gettleman, -A., Massie, -S. T., and Jiang, -J. H.: Transport above the Asian summer monsoon anticyclone inferred from Aura Microwave Limb Sounder tracers, *J. Geophys. Res.*, 112, D16309, doi:doi:10.1029/2006JD008294, 2007.
- Park, -M., Randel, -W. J., Emmons, -L. K., Bernath, -P. F., Walker, -K. A., and Boone, -C. D.: Chemical isolation in the Asian-Asian monsoon anticyclone observed in Atmospheric Chemistry Experiment (ACE-FTS) data, *Atmos. Chem. Phys.*, 8, 757–764, doi:, 2008.
- Park, -M., Randel, -W. J., Emmons, -L. K., and Livesey, -N. J.: Transport pathways of carbon monoxide in the Asian summer monsoon diagnosed from Model of Ozone and Related Tracers (MOZART), *J. Geophys. Res.*, 114, D08303, doi:doi:10.1029/2008JD010621, 2009.
- Ploeger, -F., Günther, -G., Konopka, -P., Fueglistaler, -S., Müller, -R., Hoppe, -C., Kunz, -A., Spang, -R., Grooß, -J.-U., and Riese, -M.: Horizontal water vapor transport in the lower stratosphere from subtropics to high latitudes during boreal summer, *J. Geophys. Res.*, 118, 8111–8127, doi:doi:10.1002/jgrd.50636, 2013.
- Ploeger, F., Gottschling, C., Griebßbach, S., Grooß, J.-U., Günther, G., Konopka, P., Müller, R., Riese, M., Stroh, F., Ungermann, J., Vogel, B., and von Hobe, M.: On deducing the transport barrier in the Asian summer monsoon anticyclone based on isentropic PV-gradients, *Atmos. Chem. Phys. Discuss.*, submitted, 2015.

- Pommrich, R., Müller, R., Grooß, J.-U., Konopka, P., Ploeger, F., Vogel, B., Tao, M., Hoppe, C. M., Günther, G., Spelten, N., Hoffmann, L., Pumphrey, H.-C., Viciani, S., D'Amato, F., Volk, C. M., Hoor, P., Schlager, H., and Riese, M.: Tropical troposphere to stratosphere transport of carbon monoxide and long-lived trace species in the Chemical Lagrangian Model of the Stratosphere (CLaMS), *Geosci. Model Dev.*, 7, 2895–2916, doi:10.5194/gmd-7-2895-2014, 2014.
- ~~Popovic, J. M. and Plumb, R. A.: Eddy shedding from the upper-tropospheric Asian monsoon anticyclone, *J. Atmos. Sci.*, 58, 93–104, 2001.~~
- Randel, W. J. and Park, M.: Deep convective influence on the Asian summer monsoon anticyclone and associated tracer variability observed with Atmospheric Infrared Sounder (AIRS), *J. Geophys. Res.*, 111, D12314, doi:10.1029/2005JD006490, 2006.
- Randel, W. J., Park, M., Emmons, L., Kinnison, D., Bernath, P., Walker, K. A., Boone, C., and Pumphrey, H.: Asian monsoon transport of pollution to the stratosphere, *Science*, 328, 611–613, doi:10.1126/science.1182274, 2010.
- Riese, M., Ploeger, F., Rap, A., Vogel, B., Konopka, P., Dameris, M., and Forster, P.: Impact of uncertainties in atmospheric mixing on simulated UTLS composition and related radiative effects, *J. Geophys. Res.*, 117, D16305, doi:10.1029/2012JD017751, 2012.
- Rosenlof, K. H., Tuck, A. F., Kelly, K. K., Russell III, J. M., and McCormick, M. P.: Hemispheric asymmetries in the water vapor and inferences about transport in the lower stratosphere, *J. Geophys. Res.*, 102, 13213–13234, 1997.
- Sander, S. P., Friedl, R. R., Barker, J. R., Golden, D. M., Kurylo, M. J., Wine, P. H., Abbatt, J. P. D., Burkholder, J. B., Kolb, C. E., Moortgat, G. K., Huie, R. E., and Orkin, V. L.: Chemical Kinetics and Photochemical Data for Use in Atmospheric Studies, JPL Publication, 10-6, 2011.
- ~~Schwartz, M. J., Manney, G. L., Hegglin, M. J., Livesey, N. J., Santee, M. L., and Daffer, W. H.: Climatology and variability of trace gases in extratropical double-tropopause regions from MLS, HIRDLS and ACE-FTS measurements, *J. Geophys. Res.*, 120, 843–867, doi:, 2015.~~
- Shindell, D. T.: Climate and ozone response to increased stratospheric water vapor, *Geophys. Res. Lett.*, 28, 1551–1554, doi:10.1029/1999GL011197, 2001.
- Smith, C. A., Haigh, J. D., and Toumi, R.: Radiative forcing due to trends in stratospheric water vapour, *Geophys. Res. Lett.*, 28, 179–182, 2001.
- Solomon, S., Rosenlof, K., Portmann, R., Daniel, J., Davis, S., Sanford, T., and Plattner, G.-K.: Contributions of stratospheric water vapor to decadal changes in the rate of global warming, *Science*, 327, 1219–1223, doi:10.1126/science.1182488, 2010.

- Spang, R., Gnther, G., Riese, M., Hoffmann, L., Miller, R., and Griessbach, S.: Satellite observations of cirrus clouds in the Northern Hemisphere lowermost stratosphere, *Atmos. Chem. Phys.*, 15, 927–950, doi:10.1029/2015-
Uma, K. N., Das, S. K., and Das, S. S.: A climatological perspective of water vapor at the UTLS region over different global monsoon regions: observations inferred from the Aura-MLS and re-analysis data, *Clim. Dynam.*, 43, 407–420, doi:10.1007/s00382-014-2085-9, 2014.
- Vernier, J.-P., Thomason, L. W., and Kar, J.: CALIPSO detection of an Asian tropopause aerosol layer, *Geophys. Res. Lett.*, 38, L07804, doi:10.1029/2010GL046614, 2011.
- Vogel, B., Konopka, P., Grooß, J.-U., Müller, R., Funke, B., López-Puertas, M., Reddmann, T., Stiller, G., von Clarmann, T., and Riese, M.: Model simulations of stratospheric ozone loss caused by enhanced mesospheric NO_x during Arctic Winter 2003/2004, *Atmos. Chem. Phys.*, 8, 5279–5293, doi:10.5194/acp-8-5279-2008, 2008.
- Vogel, B., Feck, T., and Grooß, J.-U.: Impact of stratospheric water vapor enhancements caused by CH₄ and H₂ increase on polar ozone loss, *J. Geophys. Res.*, 116, D05301, doi:10.1029/2010JD014234, 2011a.
- Vogel, B., Pan, L. L., Konopka, P., Günther, G., Müller, R., Hall, W., Campos, T., Pollack, I., Weinheimer, A., Wei, J., Atlas, E. L., and Bowman, K. P.: Transport pathways and signatures of mixing in the extratropical tropopause region derived from Lagrangian model simulations, *J. Geophys. Res.*, 116, D05306, doi:10.1029/2010JD014876, 2011b.
- Vogel, B., Feck, T., Grooß, J.-U., and Riese, M.: Impact of a possible future global hydrogen economy on Arctic stratospheric ozone loss, *Energ. Environ. Sci.*, 5, 6445–6452, doi:10.1039/c2ee03181g, 2012.
- Vogel, B., Günther, G., Müller, R., Grooß, J.-U., Hoor, P., Krämer, M., Müller, S., Zahn, A., and Riese, M.: Fast transport from Southeast Asia boundary layer sources to northern Europe: rapid uplift in typhoons and eastward eddy shedding of the Asian monsoon anticyclone, *Atmos. Chem. Phys.*, 14, 12745–12762, doi:10.5194/acp-14-12745-2014, 2014.
- Webster, P. J., Magaña, V. O., Palmer, T. N., Shukla, J., Tomas, R. A., Yanai, M., and Yasunari, T.: Monsoon: Processes, predictability, and the prospects for prediction, *J. Geophys. Res.*, 103, 14.451–14.510, 1998.
- Xiong, X., Houweling, S., Wei, J., Maddy, E., Sun, F., and Barnet, C.: Methane plume over south Asia during the monsoon season: satellite observation and model simulation, *Atmos. Chem. Phys.*, 9, 783–794, doi:10.5194/acp-9-783-2009, 2009.

Yan, R.-G., Bian, J.-G., and Fan, Q.-J.: The impact of the South Asia High Bimodality on the chemical composition of the upper troposphere and lower stratosphere, *Atmos. Ocean. Sci. Lett.*, 4, 229–234, 2011.

Zhang, Q., Wu, G., and Qian, Y.: The Bimodality of the 100 South Asia high and its relationship to the climate anomaly over East Asia in summer, *J. Meteorol. Soc. Jpn.*, 80, 733–744, 2002.

Table 1. Latitude and longitude range of artificial boundary layer sources in the CLaMS model, also referred to as “emission tracers”. The geographic position of each emission tracer is shown in Fig. 1.

Emission Tracer	Latitude	Longitude
North India (NIN)	20–40° N	55–90° E
South India (SIN)	0–20° N	55–90° E
East China (ECH)	20–40° N	90–125° E
Southeast Asia (SEA)	12° S–20° N	90–155° E
Siberia (SIB)	40–75° N	55–180° E
Europe (EUR)	45–75° N	20° W–55° E
Mediterranean (MED)	35–45° N	20° W–55° E
North Africa (NAF)	0–35° N	20° W–55° E
South Africa (SAF)	36° S–0° N	7–42° E
Madagascar (MDG)	27–12° S	42–52° E
Australia (AUS)	40–12° S	110–155° E
North America (NAM)	15–75° N	160–50° W
South America (SAM)	55° S–15° N	80–35° W
<u>Tropical Pacific Ocean (TPO)</u>	<u>20° S–20° N</u>	<u>see Fig. 1</u>
<u>Tropical Atlantic Ocean (TAO)</u>	<u>20° S–20° N</u>	<u>see Fig. 1</u>
<u>Tropical Indian Ocean (TIO)</u>	<u>20° S–20° N</u>	<u>see Fig. 1</u>

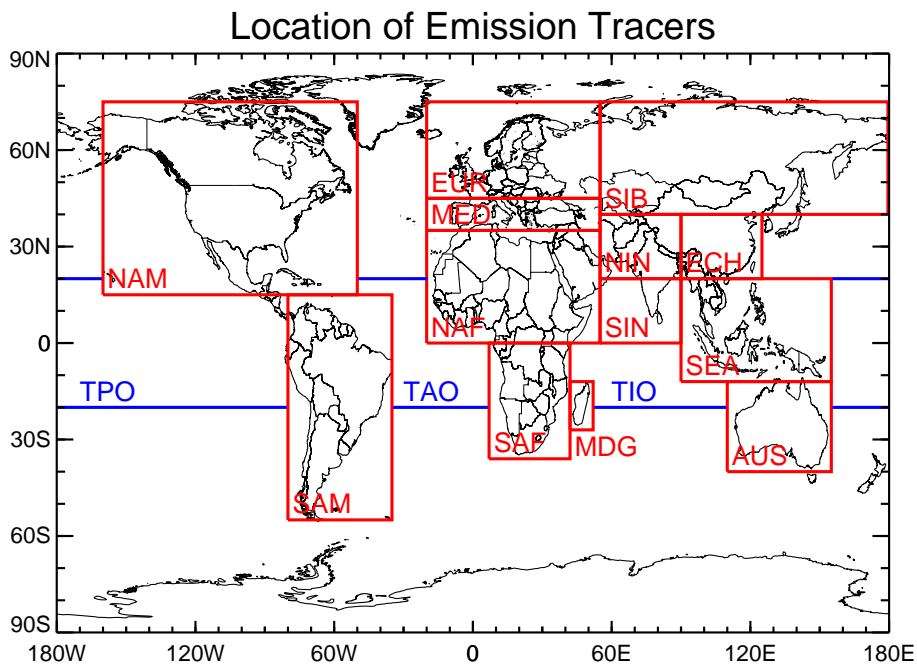


Figure 1. Global geographic ~~position~~location of artificial boundary layer source regions in the CLaMS model, also referred to as “emission tracers”. The latitude and longitude range for each emission tracer is listed in Table 1.

The horizontal distribution of the fraction of air originating in India/China (left) and PV (right) at 380 potential temperature over Asia on 1 July 2012 (top), 28 July 2012 (2nd row), 2 August 2012 (3rd row), and 8 August 2012 (bottom). Please note that the order of the colour scale for India/China (left) and PV (right) is different, so that high contributions of emission tracers for India/China and low PV are marked in red. The horizontal winds are indicated by white arrows. The black box (15–50N, 0–140E) highlights the region of the Asian monsoon anticyclone. The 4.5PVU surface marks roughly the edge of the anticyclone shown as white thick line.

The same as Fig. 2, but on 20 September 2012 (top) and on 19 October 2012 (bottom). Here for simplification, the abscissa is for the longitude range from 0 to 360 to highlight the eddy shedding event on 20 September 2012 (top) and the distribution of emission tracers for India/China after the breakup of the anticyclone on 19 October 2012 (bottom).

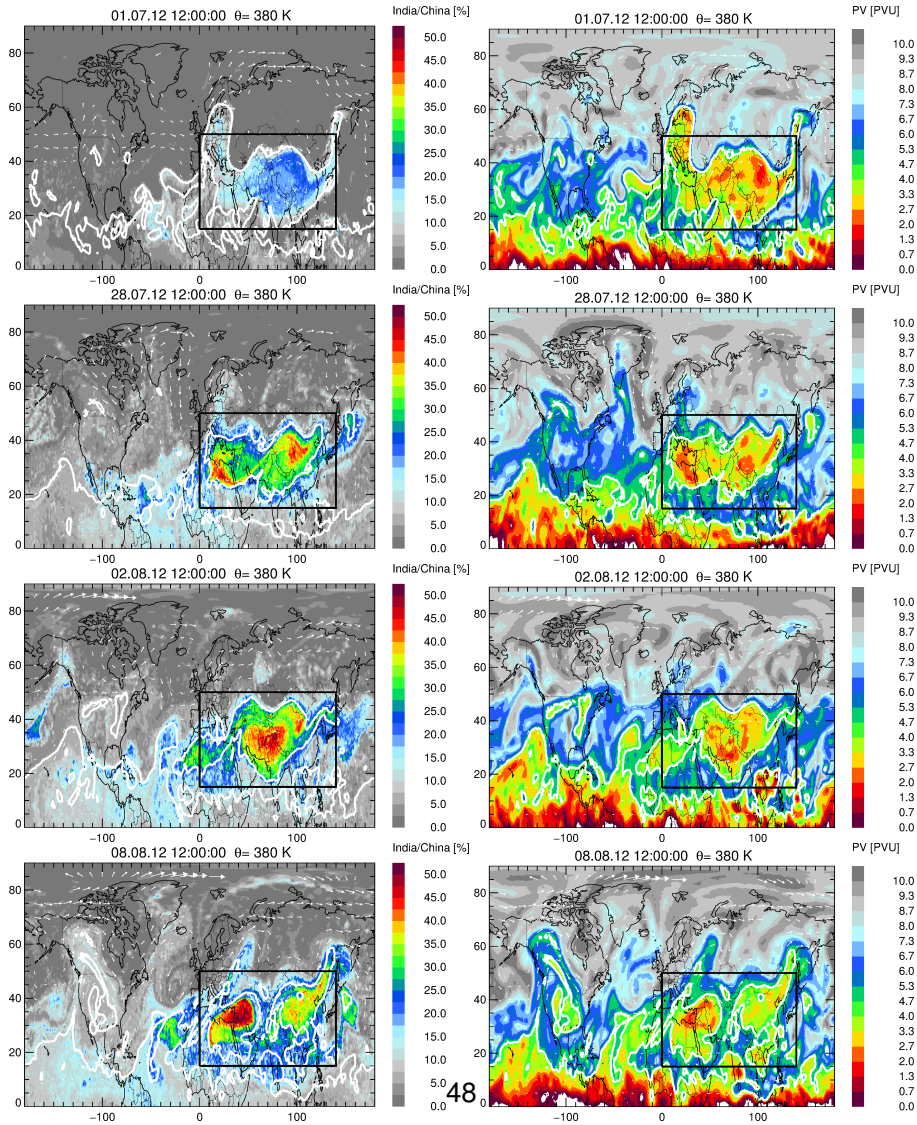


Figure 2. MLS-The horizontal distribution of the fraction of air originating in India/China (left) and CO_2 PV (right) at 380 K potential temperature over Asia on 1 July 2012 (top), 28 July 2012 (2nd row), 2 August 2012 (3rd row), and 8 August 2012 (bottom) at 380 potential temperature. Please note that the order of the colour scale for India/China (left) and PV (right) is different, so that low-ozone and high mixing-ratios-contributions of emission tracers for India/China and low PV are marked in red. The horizontal winds are indicated by white arrows. The black box-rectangle (15–50° N, 0–140° E) highlights the region of the Asian monsoon anticyclone. The 4.5 PVU surface marks roughly the edge of the anticyclone shown as white thick line.

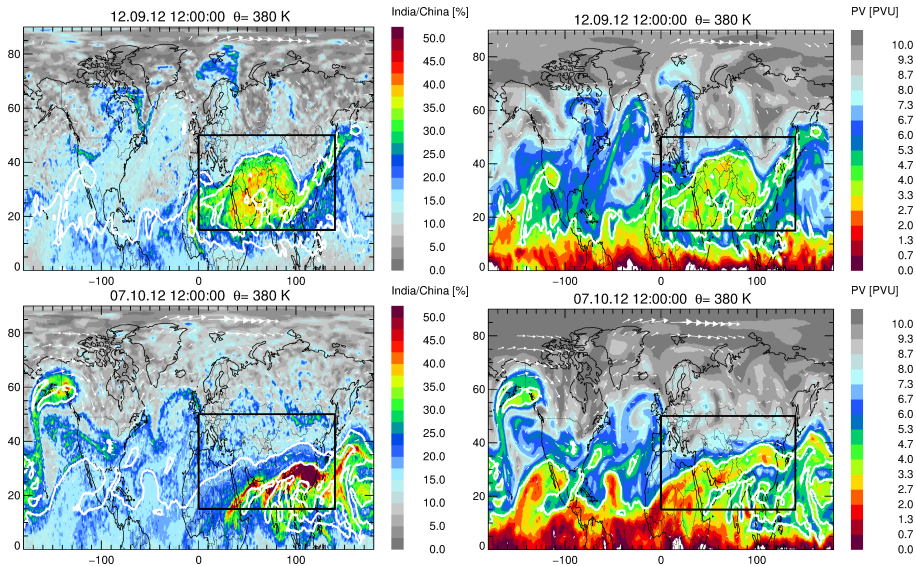


Figure 3. The same as Fig. ???, but on 2012 September 2012 (top) during the late-phase of the anticyclone and on 197 October 2012 (bottom) –Here for simplification, showing the abscissa is distribution of emission tracers for India/China after the longitude range from 0 to 360 to highlight the distribution-breakup of the anticyclone.

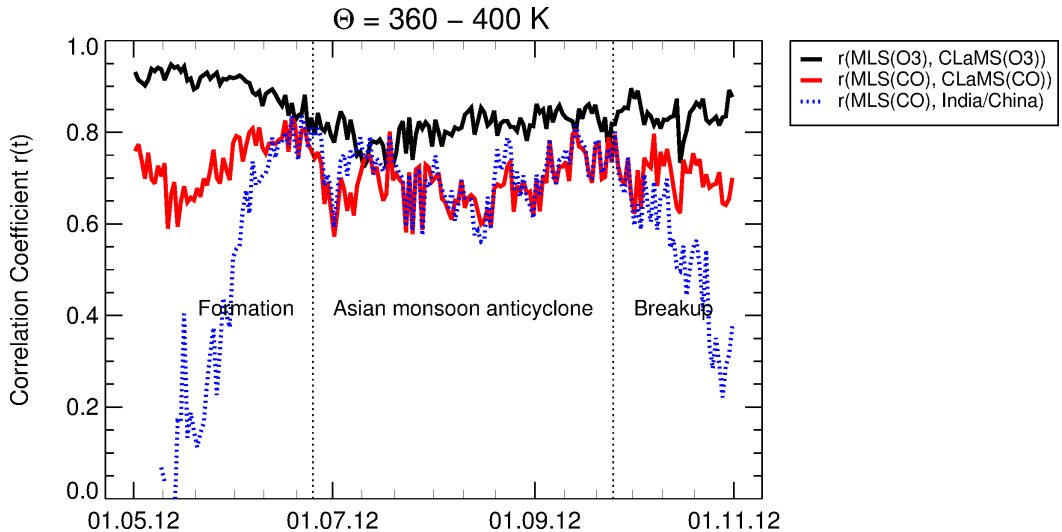


Figure 4. Correlation coefficients depending on time for tracer correlations patterns between MLS O_3 and CLaMS O_3 (black), between MLS CO and CLaMS CO during the eddy shedding event on 20 September 2012 (top red), and between MLS CO and after the breakup CLaMS emission tracer for India/China (blue) for levels of the anticyclone on 19 October 2012 (bottom) see text for more details) in a region between 15 and 50° N and 0 and 140° E (shown as black rectangle in Fig. 2 and 3).

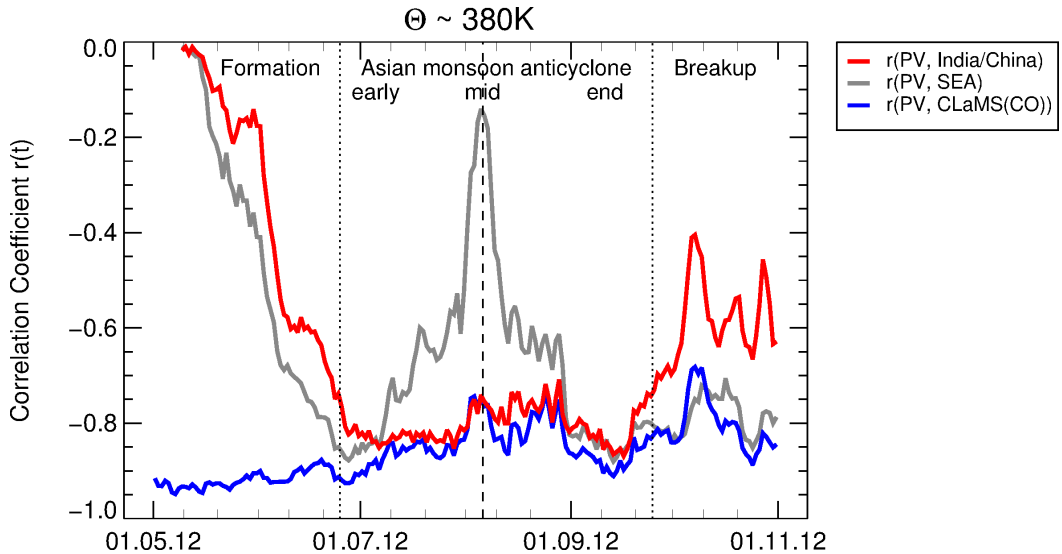
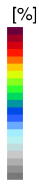
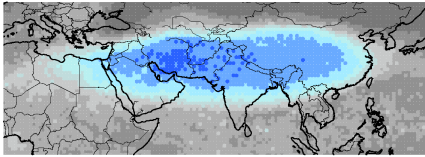
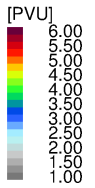
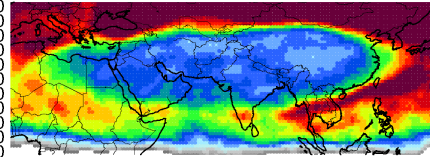


Figure 5. The number of days (N) time dependent correlation coefficients for the spatial distribution between PV and the emission tracer for India/China (red), the emission tracer for Southeast Asia (grey), and CLaMS CO (blue) at 380 K potential temperature (top panel; see text for more details) calculated in latitude-longitude bins (of 2.5° a region between 15° and 50° longitude \times 1.0° N and 0° and 140° latitude) at 380° E (± 1 shown as black rectangle in Fig. 2 and 3) with

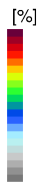
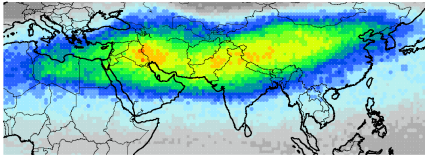
India_China 120625 – 120706 at 380K



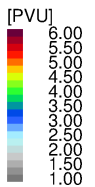
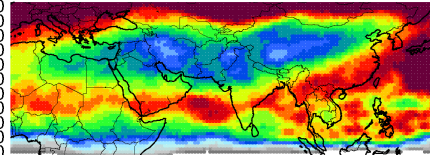
PV 120625 – 120706 at 380K



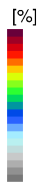
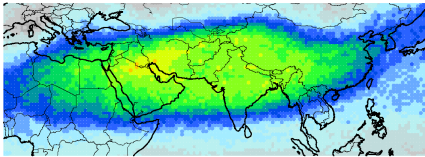
India_China 120728 – 120808 at 380K



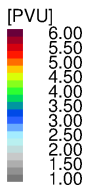
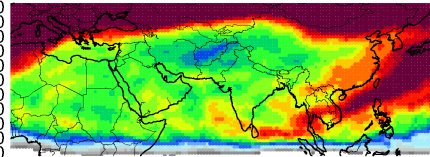
PV 120728 – 120808 at 380K



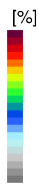
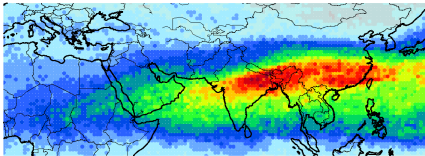
India_China 120901 – 120912 at 380K



PV 120901 – 120912 at 380K



India_China 121001 – 121012 at 380K



PV 121001 – 121012 at 380K

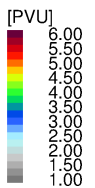
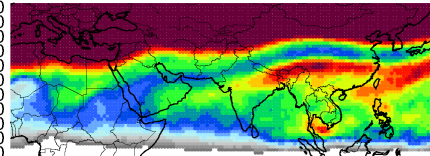


Figure 6. Twelve-day mean values of the contributions-contribution of the emission tracers-tracer for India/China larger than 35 for July/August (left) and September/October PV (right) 2012. The longitudinal dependence during four different phases of the Asian monsoon anticyclone: early-phase (bottom panel/top), mid-phase (2nd row), end-phase (3rd row) of the occurrence of days with contributions of emission tracers for India/China larger than 35 (here “counts” is anticyclone and after the number of days summarised over all latitude bins for one longitude bin: countsbreakup $(\phi) = \sum_{\lambda=15^{\circ}}^{\lambda=50^{\circ}} N(\phi)$ bottom).

Figure 7. The horizontal distribution of the fraction of air originating in (left) North India (NIN) and (right) Southeast Asia (SEA) at 380 K potential temperature over Asia on 1 July 2012 (top), on 2 August 2012 (2nd row), 8 August 2012 (3rd row) and ~~20 September 2012 (bottom)~~. ~~Note that for simplification, the abscissa for the 2012 September 2012 (bottom) is for the longitude range from 0 to 360 to highlight the eddy shedding event.~~ The horizontal winds are indicated by white arrows. The black ~~box~~ rectangle (15–50° N, 0–140° E) highlights the region of the Asian monsoon anticyclone. The 4.5 PVU surface marks roughly the edge of the anticyclone shown as white thick line.

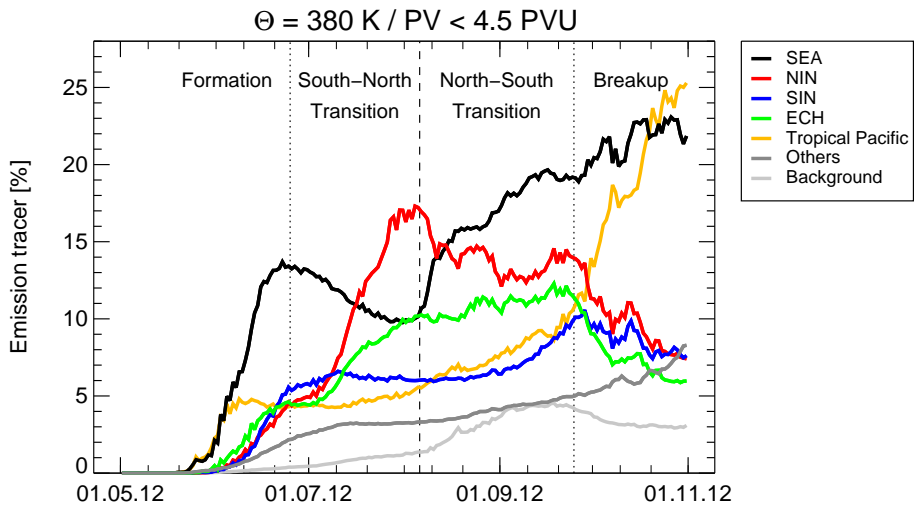


Figure 8. Temporal evolution of different emissions tracers from Southeast Asia (SEA, black), North India (NIN, red), South India (SIN, blue), East China (ECH, green), Tropic Pacific Ocean (yellow) and from all other land masses + Tropic Atlantic/Indian Ocean (others, yellowdark grey) within the Asian monsoon anticyclone at 380 K from Mai 2012 until end of October 2012. Contributions of boundary sources not considered in the defined emissions tracers listed in Table 1 are summarised as background (light grey). The shown percentages are mean values calculated for air masses in Asia in the region between 15 and 50° N and 0 and 140° E at 380 ± 0.5 K (see black box-rectangle in Fig. 7) with PV values lower than 4.5 PVU that marks the edge of the anticyclone.

The horizontal distribution of the fraction of air originating in India/China at 360(left), 380(middle), 400(right) potential temperature over Asia on 1 July (top), 2 August (2nd row), 8 August (3rd row), and 20 September (bottom) 2012. The horizontal winds are indicated by white arrows. The black box (15–50N, 0–140E) highlights the region of the Asian monsoon anticyclone. The 2, 4.5, and 9PVU surface marks roughly the edge of the anticyclone at 360, 380, and 400 shown as white thick line.

The horizontal distribution of the fraction of air originating in Southeast Asia at 360(left), 380(middle), 400(right) potential temperature over Asia on 1 July (top), 2 August (2nd row), 8 August (3rd row), and 20 September (bottom) 2012. The horizontal winds are indicated by white arrows. The black box (15–50N, 0–140E) highlights the region of the Asian monsoon anticyclone. The 2, 4.5, and 9PVU surface marks roughly the edge of the anticyclone at 360, 380, and 400 shown as white thick line.

Latitude-height cross-section of the Northern Hemisphere including the Asian Monsoon area ($\approx 15\text{--}35\text{N}$) at 80E longitude of (a) static stability (N^2), (b) the fraction of air originating in India/China (here the sum of North India (NIN), South India (SIN), and East China (ECH)), the fraction of air originating in (c) Southeast Asia (SEA) and in (d) Siberia (SIB). The corresponding levels of potential temperature are marked by thin white lines. The 380 surface is highlighted in purple to illustrate the position of the horizontal cross-sections shown in Figs. 3 and 7. Further, the thermal tropopause (black dots) and the 4.5PVU surface (thick white lines) are shown. The wind velocities are shown as black lines. The different emission tracers are initialised 2–3 above surface following orography indicated by the orange line (corresponding to ζ lower than 120).